Battelle

Final Report No. 13-002

Final Report

Models for Predicting Failure Stress Levels for Defects Affecting ERW and Flash-Welded Seams

(with an addendum by Brian Leis presenting Battelle's experience with the PAFFC model)

J. F. Kiefner and K. M. Kolovich

January 3, 2013

Kiefner & Associates, Inc.
585 Scherers Court
Worthington, Ohio 43085

(614) 888-8220
www.kiefner.com

0533-1101

Intentionally blank

Final Report No. 13-002

Final Report

on

MODELS FOR PREDICTING FAILURE STRESS LEVELS FOR DEFECTS AFFECTING ERW AND FLASH-WELDED SEAMS

(with an addendum by Brian Leis presenting Battelle's experience with the PAFFC model)

to

BATTELLE

AS THE DELIVERABLE OF SUBTASK 2.4 ON
U.S. DEPARTMENT OF TRANSPORTATION
OTHER TRANSACTION AGREEMENT NO. DTPH56-11-T-000003

January 3, 2013

by

J. F. Kiefner and K. M. Kolovich

Kiefner and Associates, Inc.
585 Scherers Court
Worthington, Ohio 43085

0533-1101

DISCLAIMER

This document presents findings and/ or recommendations based on engineering services performed by employees of Kiefner and Associates, Inc. The work addressed herein has been performed according to the authors' knowledge, information, and belief in accordance with commonly accepted procedures consistent with applicable standards of practice, and is not a guaranty or warranty, either expressed or implied.

The analysis and conclusions provided in this report are for the sole use and benefit of the Client. No information or representations contained herein are for the use or benefit of any party other than the party contracting with KAI. The scope of use of the information presented herein is limited to the facts as presented and examined, as outlined within the body of this document. No additional representations are made as to matters not specifically addressed within this report. Any additional facts or circumstances in existence but not described or considered within this report may change the analysis, outcomes and representations made in this report.

Executive Summary

The work described herein is part of a comprehensive study of ERW seam integrity and its impact on pipeline safety. The objective of this part of the work is to identify appropriate defect-assessment models for the various kinds of ERW seam defects. Such models are needed to calculate failure stresses of ERW seam defects located and characterized by in-line inspections with crack-detection tools. The calculated failure stresses are used to identify, examine, and repair defects that could cause a pipeline to fail.

This document presents an analysis of two known defect assessment methods in an effort to find suitable ways to satisfactorily predict the failure stress levels of defects in or adjacent to ERW or flash-welded line pipe seams. The models examined are the Modified LnSec equation and the Raju /Newman equation. The Modified LnSec equation is an empirical model that has been shown to work well for predicting the failure stress levels of defects in conventional line pipe materials that behave in a ductile manner. The Raju/Newman equation is a variation of the classic fracture mechanics equation that is based on the concept of a crack failing in a brittle manner when the applied stress causes the stress intensity factor, K, to reach a critical value. Calculations of failure stresses using these two models are compared to actual failure stresses observed for various seam defects in operating pipelines, in pipelines subjected to hydrostatic tests, and in burst tests conducted on pieces of pipes removed from service. The data presented herein show that both equations have their uses depending on the circumstances.

Of the four types of ERW seam defects considered herein, two types, cold welds and selective seam weld corrosion, reside in the bondlines of ERW seams. In the cases of LF-ERW, DC-ERW, and flash- welded pipe, the bondline regions tend to be prone to brittle fracture in the presence of a defect. For these types of defects, the data examined herein suggest that the Raju/Newman model provides the best means of predicting a conservative value of failure stress.

The other two types of ERW seam defects considered herein, hook cracks and defects that fail after being enlarged by pressure-cycle-induced fatigue, tend to be located in the zone of heat-affected base metal near the bondlines of ERW seams. Even in LF-ERW, DC-ERW, and flash-welded materials, these zones tend to exhibit fracture behavior that is ductile as long as the fractures do not jump to the bondlines. For these types of defects the data examined herein suggest that, as long as the fracture does not jump into the bondline, the Modified LnSec equation tends to give reasonable predictions of the actual failure stress levels of the defects.

The conclusions that arise from this study are as follows.

1. Defects in the bondlines of LF-ERW, DC-ERW, and flash-welded seams such as cold welds and selective seam weld corrosion tend to fail in a brittle manner. Therefore, it is inappropriate to use a ductile fracture model to predict their failure stresses. A more appropriate model would be one that is tailored to predicting brittle fracture initiation. The Raju/Newman equation was shown herein to predict lower-bound estimates of the actual failure stresses of bondline defects when used with an appropriate toughness level.
2. The Raju/Newman equation when used with a fracture toughness level of 22.4 $ksi\sqrt{inch}$ (corresponding to a Charpy energy of 4 ft lb) was found to give lower-bound estimates of the failure stresses of 21 cold weld defects[1].
3. The Raju/Newman equation when used with a fracture toughness level of 5.2 $ksi\sqrt{inch}$ corresponding to a Charpy energy of 0.4 ft lb) was found to give lower-bound estimates of the failure stresses of 12 selective seam weld corrosion defects.
4. Defects in the heat-affected base metal near LF-ERW, DC-ERW, and flash welded seams such as hook cracks and fatigue cracks tend to fail in a ductile manner unless the base metal itself is prone to brittle fracture initiation or the fracture jumps into the bondline. Therefore, it may be appropriate in certain circumstances to use a ductile fracture model to predict their failure stresses. The Modified LnSec equation is one such model. Other models that likely would work equally well are PAFFC, CorLas™, or an API 579, Level II analysis.
5. The Modified LnSec equation when used with the base metal Charpy energy was found to give reasonable (and often over-conservative) predictions of the failure stress levels of 39 of 59 hook cracks. The behavior of each of the remaining 20 defects was insufficiently ductile to permit the use of the Modified LnSec equation. As explained in Conclusion 7 below, the failure pressures of these brittle or semi-brittle behaving defects were predicted using the Raju/Newman equation.
6. The Modified LnSec equation when used with a Charpy energy of 15 ft lb was found to give reasonable (and often over-conservative) predictions of the failure stress levels of 31 of 32 fatigue-enlarged defects[2].

[1] The fracture toughnesses and the associated values of Charpy energy stated in Conclusions 2, 3, and 7 were back-calculated from the failure pressures and dimensions of defects that caused actual pipeline service and test failures using the Raju/Newman equation. No attempt was made to directly measure the Charpy energy levels of the seams involved. The significance of the back-calculated values is that they represent the actual full-scale behavior of typical vintage ERW seams. An analyst should be able to use these values to estimate the worst-case effects of anomalies found by in-line inspection without having to know the actual toughness of a particular seam.

[2] The Charpy energies stated in Conclusion 6 were back-calculated from the failure pressures and dimensions of fatigue-enlarged defects that caused actual pipeline service and test failures using the Modified LnSec equation. No attempt was made to directly measure the Charpy energy levels of the seams involved. The significance of the back-calculated values is that they represent the actual full-scale behavior of typical vintage ERW seams. An analyst should be able to use these values to estimate the worst-case effects of fatigue-enlarged anomalies found by in-line inspection without having to know the actual toughness of a particular seam.

7. Where a hook crack resided in a brittle material or where the fracture of a hook crack jumped into the bondline of an LF-ERW, DC-ERW, or flash-welded seam, the Raju/Newman equation used with a toughness of level of 22.4 $ksi\sqrt{inch}$ (corresponding to a Charpy energy of 4 ft lb) was found to give lower-bound estimates of the failure stress.
8. The Raju/Newman equation is probably not a suitable model to use for calculating failure stress levels for fatigue-enlarged anomalies near ERW seams because such flaws tend to fail in a ductile mode.
9. The toughness of an ERW seam within a single piece of pipe can vary significantly from point to point along the seam.
10. The use of lower-bound estimates of failure stress is permissible for prioritizing ILI crack-tool anomalies for excavation and examination. Such lower-bound estimates are not appropriate for calculating the remaining lives of unexamined defects or defects that have barely survived a hydrostatic test. Appropriate methods for calculating remaining lives are being considered in a companion study under Subtask 2.5 of this project.
11. The use of lower-bound estimates or conservative models for predicting failure stress likely will result in excavations and examinations of many anomalies that are non-injurious along with those that are found to be injurious and need to be repaired.

The details of how these results might affect the use of ILI crack-detection tools for ERW seam integrity assessments appear in the "Discussion" section of this document.

Intentionally blank

TABLE OF CONTENTS

LIST OF FIGURES

LIST OF TABLES

Intentionally blank

Models for Predicting Failure Stress Levels for Defects Affecting ERW and Flash-Welded Seams

(with an addendum by Brian Leis presenting Battelle's experience with the PAFFC model)

J. F. Kiefner and K. M. Kolovich

INTRODUCTION

This document presents an analysis of two known defect assessment methods in an effort to find suitable ways to satisfactorily predict the failure stress levels of defects in or adjacent to ERW or flash-welded line pipe seams. The models to be examined are the Modified LnSec equation and the Raju /Newman equation. Calculations of failure stresses using these two models are compared to actual failure stresses observed for various seam defects in operating pipelines, in pipelines subjected to hydrostatic tests, and in burst tests conducted on pieces of pipes removed from service.

Acknowledgement

The authors greatly appreciate the efforts of Brian Leis in providing special insights concerning the subject of defects in ERW seams. Leis' observations made a valuable contribution to this effort, and the document he prepared on the subject is attached herewith as Appendix A.

BACKGROUND

The need for a model to predict the failure stress levels of ERW seam defects is twofold. First, pipeline operators must respond to the results of seam integrity assessments using ILI crack-detection tools which provide the locations, depths, and lengths of seam anomalies. The rational way for an operator to respond is to prioritize the detected anomalies by their estimated severity, so that the most injurious anomalies are repaired first followed by less injurious anomalies. Second, the operator must be able to predict remaining times to failure for those anomalies that are not repaired, so that a subsequent integrity assessment can be made in a timely manner to prevent the growing anomalies from failing in service. In the case of hydrostatic testing, the test-pressure-to-operating-pressure ratio establishes an initial margin of safety irrespective of the sizes of defects or the material properties, but the operator must calculate remaining lives of anomalies that could have survived the test to know when to test again. In either case, a reliable failure-stress-versus-defect-size model and knowledge of the relevant material properties are necessary for calculating failure stress levels of anomalies. However, as Leis points out in Appendix A of this document, a model that gives conservative answers for the prioritization of

ILI anomalies will tend to give un-conservative answers for predicting remaining times to failure. Therefore, in this Subtask 2.4 document, the effort is focused on a model for conservatively predicting the failure stress levels of ILI-detected anomalies based on the ILI-provided dimensions of the anomalies for the purpose of prioritizing excavations. The question of a suitable model for evaluating remaining lives of anomalies that are left unrepaired after a seam-integrity assessment will be addressed in a separate Subtask 2.5 document.

Traditionally, such as in the case of corrosion-caused metal loss, responding to the anomalies in order according to their severity as calculated by a suitable failure stress model has been shown to be an effective means of assuring pipeline integrity and an effective means of forecasting when the next assessment is needed to prevent a failure from an anomaly growing at a known rate. Attempts to apply the same approach to ERW seam anomalies suggest that this may not be as straightforward as it is for corrosion anomalies. The challenges with respect to calculating failure stress levels for ERW and flash-welded seam defects are as follows:

- Defects in low-frequency-welded ERW (LF-ERW) seams, direct-current-welded ERW (DC-ERW), and flash-welded seams often fail in a brittle manner. Ductile-fracture-initiation models that have been proven to work reasonably well for predicting failure stress levels for defects in the base metal, may not work well in a material that tends to fail in a brittle manner.
- The toughness of the material which constitutes the bondline of an LF-ERW, DC-ERW, or flash-welded seam and possibly the heat-affected zone as well is often much lower than that of the surrounding base metal. Moreover, the toughness of such regions is difficult to measure and may vary significantly along the seam even within a single piece of pipe. The lowest toughness levels appear to be associated with defective seams where cold welds or stitching may be present. As will be shown in this document lower bound values of toughness for such seams can be inferred from actual pipeline service and hydrostatic test failures.

The work described in this document represents an attempt to overcome these challenges, so that pipeline operators will be better able to make decisions regarding the dispositions of particular seam anomalies detected by ILI.

In a previous report on Subtask 1.4 of this project "ERW and Flash Weld Seam Failures"[i], attempts were made to estimate the actual failure stress levels of seam defects using the ductile fracture initiation model, Modified LnSec equation[ii]. As noted in Reference 1, there was poor agreement in many cases between the predicted and the actual values. Factors that contributed to the poor agreement included the lack of knowledge of the effective toughness of the material local to the bondline regions of the welds, the difficulty of modeling the shapes of the defects, and likelihood that some of the defects may have failed in a brittle manner not appropriately modeled by the Modified LnSec equation. As detailed in Appendix A to this document, Leis demonstrates similar difficulties using the ductile fracture initiation model, PAFFC[iii].

In this document the primary mission is to determine whether or not known models can be used to make reliable predictions of failure stress levels of defects in or adjacent to ERW seams. Such models are essential for prioritizing responses to anomalies located by ILI crack-detection tools. At the current time, it is believed that the method most commonly used by the ILI vendors is an API 579[3], Level II[iv] analysis based on the failure assessment diagram (FAD) concept[v]. The FAD concept considers the possibility that a defect might fail in either an entirely ductile mode (plastic collapse), an entirely brittle mode (elastic fracture), or somewhere between these two extremes (elastic-plastic fracture). One part of a FAD calculation considers the ratio of effective tensile stress at the tip of the crack to the "flow stress" of the material to determine whether or not a plastic collapse failure will occur under the applied load. This part of the calculation could be done by any proven ductile fracture model such as PAFFC, CorLas™[vi] or the Modified LnSec equation. The other part of a FAD calculation considers the ratio of the effective stress intensity factor at the tip of the crack to the critical stress intensity factor at which elastic (brittle) failure is predicted. This part of the calculation is made using a brittle fracture model such as the Raju/Newman model[vii].

ILI vendors typically use a single level of toughness to calculate the failure stresses for all detected and sized anomalies. Anomalies are then prioritized for excavation and examination on the basis of the calculated failure stresses. The main difficulties with this process for assessment of defects in ERW seams are that the toughness of the material is usually not known and that toughnesses are likely to vary from one batch of pipe to another and even along the seam of a single piece of pipe. The fact that ILI vendors have used single levels of toughness that invariably lead to predictions of elastic-plastic failure means that the possibility of brittle fracture is often overlooked.

MODELS FOR DUCTILE AND BRITTLE FRACTURE BEHAVIOR

The equations for both the Modified LnSec model and the Raju/Newman model are given in Appendix B. Brief discussions of the origins of these equations are as follows.

[3] API 579-2/ASME FFS-1 – Fitness-for-Service, 2009

The Modified LnSec Equation

The most important component of the Modified LnSec model is a surface-flaw failure equation developed empirically by Maxey on the basis of experiments on stainless steel pressure vessels[viii,ix]. Maxey earlier had identified that the "Folias" equation[x] could be used to accurately predict the failure stress of a "through-wall" axially-oriented defect in a pressure vessel for a material like stainless steel where failure by plastic collapse predominates. Maxey's surface-flaw equation, which embodied a "Folias" factor to account for the effects of flaw length, provided satisfactory predictions of failure stresses for very-high-toughness materials.

When applied to surface-flaws in line pipe materials of pre-1970-vintage, Maxey's surface flaw equation tended to over-estimate the failure stresses of defects. As a result he developed a correction for his surface flaw equation to cover materials with less-than-optimum toughness using the "Dugdale" model[xi] for critical crack opening displacement and Charpy V-notch upper shelf energy to represent ductile toughness. This equation was originally known as the NG-18 surface flaw equation or the LnSec equation. Later, Kiefner offered an empirical correction[xii] to bring the predictions of the model for failure of shallow flaws into better alignment with full-scale test data and the predictions of other ductile fracture initiation models such as PAFFC and CorLas™. The name of the model was changed at that time to the Modified LnSec model. The key aspect of the Modified LnSec equation (and other ductile fracture models) is that it is based on the assumption that a defect in a given material will fail by plastic collapse or elastic-plastic fracture rather than by elastic (brittle) fracture. Because the Modified LnSec model is an empirical model that was validated against a particular set of full-scale tests[ii], it may not be appropriate for materials that exhibit Charpy upper shelf energies below 15 ft lb, nor should it be used for materials that exhibit clearly brittle fracture initiation behavior.

The format of the Modified LnSec equation used in the calculations herein is the "elliptic c-equivalent" format as explained in Appendix A. This format utilizes the length and depth of the defect as measured on the fracture surface, and it is assumed that the defect is semi-elliptically-shaped. The length of the defect is taken as the major axis of the ellipse and the depth is taken as half the minor axis. The defect is then assumed to have an area equal to the depth of the defect times its equivalent length where the equivalent length is $\pi/4$ times the overall length.

The Raju/Newman Model

The Raju/Newman model is based on the classic elastic fracture concept of failure being defined by a critical level of "stress intensity factor". The stress intensity factor comes from a mathematical representation of the singularity at the tip of an infinitely sharp crack. At a critical value of the stress intensity factor, the crack in a brittle material may suddenly propagate in an unstable manner. The concept was first advanced by Griffith[xiii] in 1920 based on experiments with glass specimens. Later, Irwin[xiv] introduced the concept in the form of the following equation.

$$K = \sigma\sqrt{\pi c} \quad \textbf{Equation 1}$$

where:
K is the stress intensity factor at the tip of an infinitely sharp through-wall crack in an infinitely wide flat plate, $ksi\sqrt{inch}$
σ is the uniform stress perpendicular to the plane of the crack, ksi
c is half of the crack length, inches

Failure is said to occur when the stress intensity factor reaches a critical value referred to as K_{Ic}.[4]

K_{Ic} is a material property, the elastic "fracture toughness" of the material. K_{Ic} can be measured for many materials including low-carbon steels if the material is tested in the form of a special specimen at a temperature below its ductile-to-brittle fracture initiation transition temperature. In most cases a line pipe material will not fail at the stress level predicted by Equation 1 even if a valid K_{Ic} has been determined for the material. The reason is that the ductile-to-brittle fracture initiation transition temperature for the parent material of normal line pipe is well below typical ambient temperatures. Instead, a flaw in the body of a line pipe material fails at a much higher level than that predicted by Equation 1 because the failure mode involves ductile tearing at the tip of the flaw. The important exception relevant to this document is that some types of defects in bondline regions of LF-ERW, DC-ERW, or flash-welded materials appear to behave in the manner anticipated by Equation 1. It is believed that under such circumstances the failure stress level may be better predicted by Equation 1 than by any model where ductile tearing of the flaw is anticipated before failure.

Raju and Newman used finite element analysis methods to derive stress intensity factors for flaws in all sorts of structural shapes and components allowing the technical community to extend the concept embodied in Equation 1 well beyond the simple flat plate geometry. They then used curve-fitting techniques to create equations for various complex geometries. Their equation for axial surface flaws in pressurized cylinders is presented in Appendix B. To facilitate the use of the Raju/Newman model in this study, it was necessary to obtain values of fracture toughness, K_{Ic}, through a correlation between K_{Ic} and Charpy energy. The correlation

[4] K_{Ic} applies when plane-strain conditions exist. If they do not the parameter is usually referred to as K_c. K_c is used herein because line pipe is generally too thin for plane-strain conditions to exist.

chosen was taken from a well-known text book by Barsom and Rolfe[xv]. That correlation is known as the "Roberts-Newton" lower-bound correlation. It is given by the following equation.

$$K_c = 9.35CVN^{0.63}$$ **Equation 2**

where:

K_c is the fracture toughness, $ksi\sqrt{inch}$
CVN is the full-size-equivalent Charpy V-notch upper shelf energy in ft lb

It is stated in Reference 15 that this is a lower-bound correlation because it is based on initial crack extension and does not account for the increase in toughness associated with ductile crack extension. This seems appropriate for the observed brittle behavior of the typical ERW bondline material.

EVALUATIONS OF THE MODELS

The database of ERW seam failures presented in Reference 1 (the Subtask 1.4 report on ERW and flash weld seam failures) is used to assess the usefulness of the models with respect to predicting the failure of ERW seam defects. It is recalled that predictions of failure stress in Reference 1 were made exclusively with the Modified LnSec equation. The predictions were made based on anomaly dimensions taken from photographs of fracture surfaces of failed ERW seams, flow stress values derived from tensile tests, and Charpy V-notch upper shelf energies measured in the parent materials. The predicted levels of failure stress were then compared to the actual failure stress levels associated with the failures. In general, the predicted failure stresses did not compare favorably with the actual failure stresses, sometimes over-estimating the actual values and sometimes under-estimating them. Basically, there was no correlation between the predicted and the actual values. The lack of correlation between the model predictions and the actual failure stresses was attributed to the fact that parent metal properties (flow stress and Charpy energy) do not accurately reflect the properties in and near the bondline of and ERW material and to the fact that many of the failures associated with flaws in the bondline were quite brittle in nature[5]. It was noted, however, that cases of over-estimating the actual failure stress were more prevalent for anomalies located in the bondline region of the seam (i.e., cold welds

[5] In recent times there has been more focus on measuring toughness local to the bondlines and heat-affected zones of ERW seams. Unfortunately, that kind of data was not available for most of the defects in the database used in this report. Going forward, more effort should be made to obtain those toughnesses. It is expected that improved correlations between actual failure stresses and predicted failure stresses would result, at least for materials that fracture in a reasonably ductile manner.

and selective seam weld corrosion) than they were for anomalies located in the heat-affected base metal near the bondline. This is not surprising given that the heat-affected base metal region tends to have properties more nearly like those of the base metal than those of the bondline.

In the following sections, predictions of failure stress made by both the Modified LnSec equation and by the Raju/Newman equation are compared to actual failure stresses for four classes of ERW seam defects: cold welds, hook cracks, selective seam weld corrosion, and fatigue cracks. The expectation is that the bondlines in low-frequency-welded ERW (LF-ERW), dc-welded-ERW (DC-ERW), and flash-welded pipe tend to exhibit brittle fracture behavior at normal ambient temperatures. In contrast, the expectation is that the bondlines in high-frequency-welded ERW pipe (HF-ERW) tend to exhibit at least partly ductile fracture behavior at normal ambient temperatures.

Predictions of Failure Stress for Cold Weld Defects

Presented in Table 1 are 21 cases involving cold weld defects that failed. The table lists the attributes of the pipeline material, the failure stress as a percent of SMYS, the key pipe body properties, and the dimensions of the anomalies that caused the failures. In every case the failure mode was a rupture. Leaks are not considered in the analysis because the hoop stress at which a leak occurs is often uncertain, making it impossible to compare the actual failure stress to the predicted failure stress. For cross reference with the Subtask 1.4 report, the Case Number as used in that report is included as well.

Table 1. Attributes of ERW Materials and the Cold Weld Anomalies that Caused Them to Fail (the failure stress for Failure #4 is highlighted because it was at least this high, possibly higher because of a surge)

Cold Weld Failure Number	Case Number (from Reference 1)	Diameter, inches	Wall Thickness, inch	Grade	Actual Failure Stress, %SMYS	Pipe Body Properties		Anomaly Dimensions	
						Actual Yield Strength, psi	Charpy Upper Shelf Energy, ft lb (full-size equiv.)	Length, inches	Depth, inch
1	15	12.75	0.375	X52	59.2	62,500	240	8.50	0.250
2	22	6.625	0.188	X42	67.4	58,500	50	1.10	0.131
3	29	12.75	0.375	X52	71.2	71,500	240	3.00	0.125
4	31	8.625	0.156	X52	72.4	56,000	47	60.00	0.070
5	40	20	0.375	Grade B	77.8	47,900	26	1.50	0.188
6	41	20	0.375	Grade B	78.5	45,800	29	1.55	0.334
7	44	8.625	0.203	X52	79.1	56,000	31	2.50	0.100
8	45	16	0.25	X52	79.4	59,000	24	1.75	0.150
9	49	8.625	0.265	Grade B	80.6	52,900	24	1.10	0.100
10	55	10.75	0.219	X52	83.8	61,500	27	8.00	0.087
11	57	10.75	0.219	X52	85.6	65,500	52	6.25	0.065
12	58	10.75	0.219	X52	85.8	61,000	58	10.00	0.098
13	59	8.625	0.188	X52	86.0	63,500	34	4.00	0.070
14	60	22	0.344	X46	86.2	51,500	31	1.70	0.212
15	61	22	0.344	X46	86.8	55,000	18	1.15	0.137
16	67	10.75	0.219	X52	89.4	65,000	48	3.25	0.073
17	72	12.75	0.25	X46	93.8	49,100	36	8.00	0.090
18	74	12.75	0.25	X46	94.5	60,000	25	1.00	0.125
19	76	12.75	0.25	X46	94.6	47,200	29	2.00	0.118
20	77	12.75	0.25	X46	94.7	53,500	29	2.00	0.163
21	88	12.75	0.25	X46	97.9	53,500	32	1.00	0.225

For each cold weld anomaly, two calculations of predicted failure stress levels were made, one using the Modified LnSec equation with the Charpy energy measured for the pipe body material, and one using the Raju/Newman equation with the Charpy energy fixed at 4 ft lb. The reason for using the 4 ft lb value will become apparent. It is noted that the Raju/Newman equation treats flaws connected to the inside surface of the pipe slightly differently from flaws connected to the outside surface. The difference amounts to a 10% lower failure stress for a flaw if it is OD-connected as opposed to being ID-connected. Because that results in a lower failure stress prediction for OD-connected flaws, and because a conservative prediction is desired, all Raju/Newman calculations were made based the flaw being OD-connected regardless of the actual circumstances of the individual flaw.

The predicted failure stress levels for the 21 anomalies based on both models are presented in Table 2 along with the actual failure stress levels arranged in ascending order. The ratios, S_a/S_f, (actual to predicted failure stress) for each model are also given in the column next to the failure stress predicted by each model.

Table 2. Failure Stress Levels for Cold Weld Anomalies Predicted by Both Methods Compared to Actual Failure Stress Levels

Cold Weld Failure No.	Actual Failure Stress, %SMYS	Predicted Failure Stress, % SMYS			
		Modified LnSec (Using Actual Pipe Body Shelf Energy)	S_a/S_f Mod. LnSec	Raju/Newman (Using 4 ft lb Shelf Energy)	S_a/S_f Raju/ Newman
1	59.2	62.8	0.94	14.8	4.00
2	67.4	121.9	0.55	45.7	1.47
3	71.2	140.0	0.51	42.5	1.67
4	72.4	53.5	1.35	34.3	2.11
5	77.8	157.0	0.50	55.8	1.39
6	78.5	109.0	0.72	43.1	1.82
7	79.1	94.7	0.83	37.6	2.10
8	79.4	112.2	0.71	34.4	2.31
9	80.6	170.5	0.47	76.1	1.06
10	83.8	87.2	0.96	39.5	2.12
11	85.6	114.0	0.75	56.9	1.51
12	85.8	83.4	1.03	32.3	2.66
13	86.0	106.4	0.81	48.8	1.76
14	86.2	96.4	0.89	36.7	2.35
15	86.8	138.4	0.63	53.6	1.62
16	89.4	120.5	0.74	53.1	1.69
17	93.8	92.7	1.01	48.2	1.94
18	94.5	144.2	0.66	52.0	1.82
19	94.6	107.2	0.88	45.1	2.10
20	94.7	103.4	0.92	34.3	2.76
21	97.9	92.0	1.06	40.8	2.40

In the cases of both models, the predicted failure stresses for the cold weld defects appear to have no correlation to the actual failure stresses. However, the S_a/S_f levels for the Raju/Newman predictions are all greater than 1.0 indicating that they are conservative predictions.

It is suspected that the main reason for the lack of correlation between the actual and the predicted stresses for either model is that the actual effective toughnesses of the bondline regions vary, and only by coincidence would the value happen to be either the same as the pipe body toughness or the arbitrarily chosen value represented by a Charpy energy of 4 ft lb. Incidentally, the Charpy value of 4 ft lb corresponds to a K_c value of 22.4 $ksi\sqrt{inch}$ according to Equation 2. Another factor in the lack of correlation could be the fact that the shapes assumed for model analyses do not always reflect the actual shapes of the defects.

Comparisons of the actual failure stresses to the predicted failure stresses for the 21 cold welds are illustrated in Figures 1 and 2. The sloping lines represent perfect agreement between actual and predicted stresses. The dashed vertical lines represent potential acceptance limits based on a predicted failure stress of 100% of SMYS.

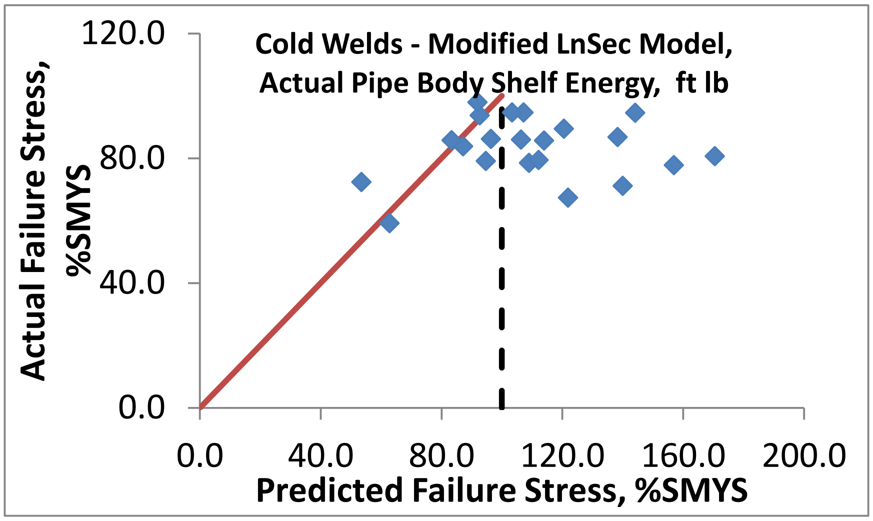

Figure 1. Comparisons of Actual to Predicted Failure Stresses for Cold Weld Anomalies Using the Modified LnSec Equation with the Actual Pipe Body Charpy Energy

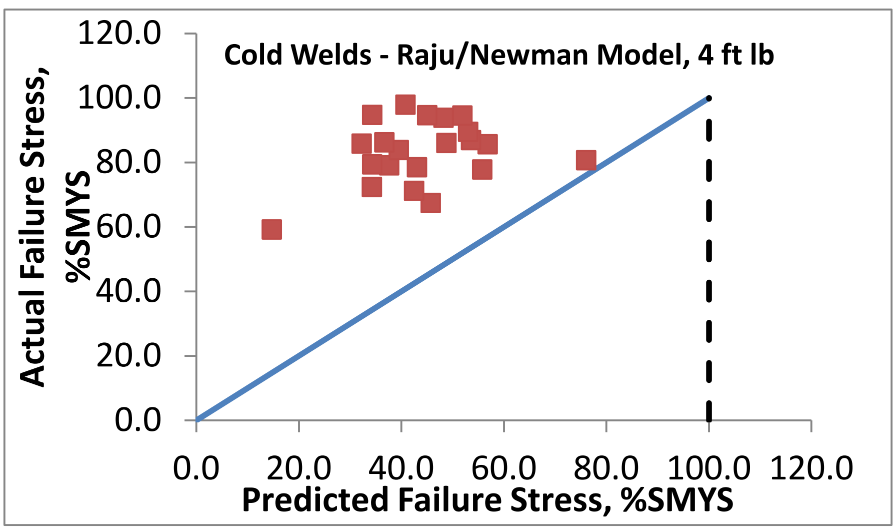

Figure 2. Comparisons of Actual to Predicted Failure Stresses for Cold Weld Anomalies Using the Raju/Newman Equation with a Charpy Energy of 4 ft lb

Very few of these comparisons resulted in agreement between the actual and the predicted failure stresses for either the Modified LnSec equation or the Raju/Newman equation. However, there is a significant difference between the comparisons based on the Modified LnSec equation and those based on the Raju/Newman equation. Whereas most of predictions using the Modified LnSec equation over-estimated the actual failure stresses by significant amounts, it is seen that all of the predictions using the Raju/Newman equation with a Charpy energy of 4 ft lb are conservative.

The tendency of the Modified LnSec equation, a ductile fracture initiation model, to over-predict the failure stresses of cold weld defects is believed to be the result of the brittle fracture initiation tendency of cold weld defects in LF-ERW, DC-ERW, and flash-welded pipe at normal ambient temperatures. In contrast, the Raju/Newman equation, which is intended to model brittle fracture initiation, appears to be capable of at least conservatively predicting the failure stress levels of cold weld defects. Better agreement between the actual and the predicted failure stresses might be obtainable if the actual effective bondline toughness were to be used. The problem is that the actual effective bondline toughness is unlikely to be known for each piece of pipe in a pipeline. However, a model such as the Raju/Newman equation could be used with a fixed level of toughness chosen intentionally to be a lower bound value to predict conservative values of failure stress. For the 21 cases examined, a level of toughness corresponding to 4 ft lb seems to fulfill that requirement.

An example of brittle fracture initiation at a cold weld (Table 1, Cold Weld Failure Number 9) is shown in Figure 3. The figure shows the two matching fracture surfaces. The dark-colored area is a cold weld (a.k.a., lack of fusion). The rust-colored areas are the fracture surfaces.

Figure 3. An Example of Brittle Fracture Initiation in Conjunction with a Cold Weld

In this case the length of the anomaly was 1.1 inch, and its depth at the deepest point was 38% of the wall thickness. Whereas, the predicted failure stress using the Modified LnSec equation with actual pipe-body Charpy energy is 170.5% of SMYS (a Grade B material with a very high actual yield strength), the predicted failure stress using the Raju/Newman equation is 76.1% of SMYS, and the actual failure stress was 80.6% of SMYS. The case corresponds to the farthest-right point in each of the two failure-stress comparison figures (Figure 1 and Figure 2). The ductile-fracture model is clearly not suitable for predicting the failure stress levels for cold weld anomalies unless the material of the bondline is capable of exhibiting ductile fracture initiation.

In 6 of the 21 cold weld failures, the failure stresses predicted by the Modified LnSec equation were not that bad compared to the actual stresses, that is, their S_a/S_f ratios ranged from 0.92 to 1.35. There are various reasons why the Modified LnSec equation appeared to give more reasonably predictions in these six cases. Cases 1 and 4 involved HF-ERW pipe where the bondline region could have had sufficient toughness to cause the failures to initiate in a ductile manner. Case 10 was a bondline defect, but apparently the material was tougher than the brittle fracture surface suggested. In Cases 12, and 17, the fractures did not lie entirely on the bondlines. Case 21 involved a very deep cold weld, where the remaining ligament was so thin that the failure occurred by ductile tearing. Nevertheless, for 15 of 21 of the cold weld defects the Modified LnSec equation gave quite un-conservative predictions of the failure stresses (S_a/S_f ratios ranging from 0.47 to 0.89). In contrast, the Raju/Newman equation used with a toughness corresponding to 4 ft lb of Charpy energy gave conservative predictions in every case.

The downside to having to use a conservative, brittle fracture initiation model is that more anomalies will not pass an acceptance limit than would be the case with a ductile fracture model. Consider the vertical dashed lines on Figure 1 and Figure 2 located at 100% of SMYS on the "Predicted Failure Stress" axis. If it is decided that all anomalies with predicted failure stress levels below 100% of SMYS must be excavated and examined, only 8 of the 21 anomalies would be excavated based on the Modified LnSec equation (the ones having predicted failure stress levels less than 100% in Table 2). In contrast, by this criterion all 21 anomalies would be excavated based on the Raju/Newman equation. As indicated in Table 2, the actual failure stress levels of all 21 anomalies were less than 100% of SMYS. One can also see from Table 2 that five of the anomalies that would not have been excavated based on the Modified LnSec equation had actual failure stresses less than 80% of SMYS. Making more excavations, by itself, does not necessarily assure greater integrity if the model used is too conservative, but in the cases of these 21 cold welds, the Raju/Newman approach does give greater assurance of pipeline integrity than the Modified LnSec equation.

Conclusions Regarding Predicting Failure Stress Levels for Cold Weld Anomalies

- Ductile fracture initiation models such as the Modified LnSec equation, PAFFC, or Corlas™ should not be used to predict failure stress levels of cold weld anomalies in LF-ERW, DC-ERW, or flash-welded seams that appear on a list of cold weld anomalies detected and sized by ILI.
- The Raju/Newman equation can be used to predict conservative failure stress levels of cold weld anomalies detected and sized by ILI. A value of toughness corresponding to 4 ft lb of Charpy energy (equal to a fracture toughness of 22.4 $ksi\sqrt{inch}$ based on Equation 2) would seem to be an appropriate value to use to assure a conservative level of predicted failure stress.
- Using the more-conservative (and more appropriate) Raju/Newman model likely will result in a pipeline operator having to do more excavations of ILI-discovered anomalies. However, the 21 examples of cold weld failures presented herein suggest that the conservatism was justified because the actual failure stresses were less than 100% of SMYS.
- As Leis has pointed out in Appendix A, a conservative approach is not appropriate for predicting the remaining lives of anomalies that have survived a particular hydrostatic test stress level. The appropriate approach for predicting the remaining lives will be presented in the Subtask 2.5 report.
- The K_r portion of a FAD calculation [6] based on an API 579-2/ASME FFS-1 – Fitness-for-Service, Level II calculation could be used in place of the Raju/Newman calculation because the two calculations give virtually the same answers if the same K_c value is used.

Predictions of Failure Stress for Hook Crack Defects

Presented in Table 3 and Table 4 are 59 cases involving hook crack defects that failed. The table lists the attributes of the pipeline material, the failure stress as a percent of SMYS, the key pipe body properties, and the dimensions of the anomalies that caused the failures. In every case the failure mode was a rupture. Leaks are not considered in the analysis because the hoop stress at which a leak occurs is often uncertain, making it impossible to compare the actual failure stress to the predicted failure stress. For cross reference with the Subtask 1.4 report, the Case Number as used in that report is included as well. Note that none of these 59 hook cracks is believed to

[6] K_r represents the ratio of the stress intensity factor associated with a particular loading and defect to the critical level of stress intensity factor at which failure will occur.

have been enlarged by pressure-cycle-induced fatigue. Hook cracks that were obviously enlarged by pressure-cycle-induced fatigue are discussed later in this report.

Table 3. Attributes of ERW Materials and Hook Crack Anomalies 1 through 30 that Caused Failures (The yellow highlighted items represent reasonable assumed values where the actual data was not provided.)

Hook Crack Failure Number	Case Number (from Reference 1)	Diameter, inches	Wall Thickness, inch	Grade	Seam Type		Pipe Body Properties		Anomaly Dimensions	
						Actual Failure Stress, %SMYS	Actual Yield Strength, psi	Charpy Upper Shelf Energy, ft lb (full-size	Length, inches	Depth, inch
1	2	12.75	0.219	X52	ERW - LF	68.3	61,500	26	7.50	0.065
2	3	16	0.312	X52	ERW - LF	68.5	52,500	29	44.00	0.125
3	4	12.75	0.281	B	ERW - LF	78.8	40,000	15	22.00	0.141
4	5	18	0.312	X46	ERW - DC	80.8	46,000	15	6.00	0.156
5	6	10.75	0.219	X52	ERW - LF	81.2	61,500	42	9.00	0.084
6	7	20	0.312	X42	ERW - DC	81.3	60,200	15	5.00	0.066
7	8	22	0.312	X46	ERW - DC	81.4	55,500	16	1.60	0.094
8	9	16	0.25	X52	ERW - LF	81.8	63,000	43	2.75	0.125
9	10	20	0.312	X42	ERW - DC	82.3	52,300	15	2.00	0.069
10	13	10.75	0.219	X52	ERW - LF	83.1	60,500	43	10.75	0.076
11	14	10.75	0.219	X52	ERW - LF	83.4	66,200	44	3.00	0.085
12	15	16	0.308	X52	ERW - HF	83.7	57,000	38	6.50	0.120
13	16	10.75	0.219	X52	ERW - LF	83.8	65,900	29	8.50	0.087
14	17	18	0.312	X46	ERW - DC	85.6	46,000	15	6.30	0.156
15	18	20	0.312	X42	ERW - DC	85.6	60,800	15	5.00	0.107
16	19	10.75	0.203	X52	ERW - HF	86.0	52,800	15	10.00	0.047
17	21	12.75	0.219	X52	ERW - LF	87.4	55,000	41	5.25	0.123
18	22	10.75	0.219	X52	ERW - LF	87.6	66,000	24	2.00	0.075
19	23	10.75	0.219	X52	ERW - LF	87.6	66,500	30	10.00	0.076
20	24	12.75	0.281	B	ERW - LF	88.2	49,600	29	7.00	0.112
21	25	12.75	0.25	X52	ERW - HF	88.3	72,000	18	8.00	0.095
22	26	10.75	0.219	X52	ERW - LF	88.4	62,000	26	7.80	0.075
23	27	18	0.312	X46	ERW - DC	88.4	46,000	15	4.25	0.062
24	28	10.75	0.203	X52	ERW - HF	89.9	54,800	15	10.00	0.098
25	31	12.75	0.281	B	ERW - LF	91.4	35,000	9	3.50	0.112
26	33	16	0.25	X52	ERW - LF	91.9	54,000	25	6.40	0.063
27	35	12.75	0.25	X52	ERW - LF	92.3	64,000	36	2.40	0.125
28	36	12.75	0.25	X52	ERW - LF	92.7	64,500	48	3.00	0.113
29	37	12.75	0.25	X52	ERW - LF	93.5	59,500	36	1.80	0.048
30	38	12.75	0.25	X52	ERW - LF	94.0	64,000	44	7.00	0.075

Table 4. Attributes of ERW Materials and Hook Crack Anomalies 31 through 59 that Caused Failures (The yellow highlighted items represent reasonable assumed values where the actual data was not provided.)

Hook Crack Failure Number	Case Number (from Reference 1)	Diameter, inches	Wall Thickness, inch	Grade	Seam Type	Actual Failure Stress, %SMYS	Pipe Body Properties: Actual Yield Strength, psi	Pipe Body Properties: Charpy Upper Shelf Energy, ft lb (full-size	Anomaly Dimensions: Length, inches	Anomaly Dimensions: Depth, inch
31	39	12.75	0.25	X46	ERW - LF	94.1	54,000	34	6.00	0.100
32	41	12.75	0.25	X52	ERW - LF	94.3	64,500	36	5.80	0.086
33	44	12.75	0.25	X52	ERW - LF	94.9	61,000	28	5.50	0.093
34	46	12.75	0.25	X52	ERW - LF	95.8	61,000	38	2.20	0.097
35	47	12.75	0.25	X46	ERW - LF	95.9	46,100	25	2.70	0.063
36	48	12.75	0.25	X52	ERW - LF	96.1	61,000	36	8.00	0.080
37	49	6.625	0.125	X60	ERW - HF	97.3	66,500	23	4.00	0.060
38	50	20	0.312	X46	ERW - DC	98.0	49,000	59	6.00	0.147
39	52	8.625	0.156	X46	ERW - LF	100.7	55,700	36	15.69	0.067
40	55	10.75	0.188	X52	ERW - HF	102.2	58,500	24	6.00	0.038
41	56	20	0.312	X52	Flash-weld	103.2	52,000	15	5.00	0.187
42	57	20	0.312	X52	Flash-weld	112.5	52,000	15	2.00	0.171
43	58	20	0.312	X52	Flash-weld	112.5	52,000	15	4.00	0.125
44	59	20	0.312	X52	Flash-weld	112.6	52,000	15	4.00	0.125
45	61	16	0.25	X42	ERW - LF	113.5	47,400	20	4.30	0.053
46	62	20	0.312	X52	Flash-weld	115.6	52,000	15	12.00	0.109
47	63	12.75	0.209	X52	ERW - LF	116.1	52,000	15	2.87	0.079
48	64	20	0.312	X52	Flash-weld	117.1	52,000	15	5.00	0.125
49	65	20	0.312	X52	Flash-weld	118.7	52,000	15	10.50	0.140
50	66	20	0.312	X52	Flash-weld	120.2	52,000	15	8.25	0.125
51	67	20	0.312	X52	Flash-weld	126.4	52,000	15	4.00	0.093
52	68	20	0.312	X52	Flash-weld	126.4	52,000	15	8.00	0.156
53	70	12.75	0.228	X52	ERW - LF	127.1	52,000	15	1.85	0.047
54	71	20	0.312	X52	Flash-weld	132.5	52,000	15	6.63	0.156
55	72	20	0.312	X52	ERW - DC	135.6	52,000	15	5.50	0.150
56	73	20	0.312	X52	ERW - DC	135.6	52,000	15	6.00	0.120
57	74	20	0.312	X52	ERW - DC	135.6	52,000	15	7.00	0.120
58	75	20	0.312	X52	Flash-weld	138.7	52,000	15	9.00	0.124
59	76	20	0.312	X52	Flash-weld	140.2	52,000	15	2.25	0.187

For each hook crack anomaly, two calculations of predicted failure stress levels were made, one using the Modified LnSec equation with the Charpy energy measured for the pipe body material, and one using the Raju/Newman equation with the Charpy energy fixed at 4 ft lb. As was the case for the cold weld defects, it will become apparent that the Raju/Newman equation provides lower bound predictions for the hook crack defects as well when used with a toughness level corresponding to a Charpy energy of 4 ft lb.

The predicted failure stress levels for the 59 anomalies are presented in Table 5 and Table 6 along with the actual failure stress levels arranged in ascending order. The ratios, S_a/S_f, (actual to predicted failure stress) for each model are also given in the column next to the failure stress predicted by each model.

Table 5. Failure Stress Levels for Hook Crack Anomalies 1 through 30 Predicted by Both Methods Compared to Actual Failure Stress Levels

Hook Crack Failure No.	Actual Failure Stress, %SMYS	Predicted Failure Stress, %SMYS			
		Modified LnSec (Using Actual Pipe Body Shelf Energy)	S_a/S_f Mod Ln/Sec	Raju/Newman (Using 4 ft lb Shelf Energy)	S_a/S_f Raju/ Newman
1	68.3	100.9	0.68	32.5	1.20
2	68.5	58.1	1.18	14.8	2.26
3	78.8	57.1	1.38	45.7	2.43
4	80.8	78.3	1.03	42.5	2.65
5	81.2	91.0	0.89	34.3	1.98
6	81.3	143.0	0.57	55.8	0.99
7	81.4	138.4	0.59	43.1	1.30
8	81.8	113.3	0.72	37.6	2.33
9	82.3	143.7	0.57	34.4	1.00
10	83.1	91.7	0.91	76.1	1.79
11	83.4	119.1	0.70	36.9	1.81
12	83.7	95.7	0.87	39.5	2.30
13	83.8	90.3	0.93	56.9	2.13
14	85.6	76.8	1.11	32.3	2.84
15	85.6	129.3	0.66	48.8	1.59
16	86.0	88.8	0.97	36.7	1.16
17	87.4	73.8	1.19	53.6	3.41
18	87.6	130.8	0.67	53.1	1.60
19	87.6	94.6	0.93	48.2	1.88
20	88.2	119.8	0.74	52.0	1.64
21	88.3	94.9	0.93	45.1	2.22
22	88.4	94.4	0.94	34.3	1.84
23	88.4	110.6	0.80	40.8	1.13
24	89.9	60.0	1.50	29.4	3.06
25	91.4	103.2	0.89	59.4	1.54
26	91.9	100.8	0.91	63.2	1.45
27	92.3	115.5	0.80	36.1	2.56
28	92.7	114.3	0.81	37.7	2.46
29	93.5	129.0	0.73	80.3	1.16
30	94.0	110.5	0.85	52.8	1.78

Table 6. Failure Stress Levels for Hook Crack Anomalies 31 through 59 Predicted by Both Methods Compared to Actual Failure Stress Levels

Hook Crack Failure No.	Actual Failure Stress, %SMYS	Predicted Failure Stress, %SMYS			
		Modified LnSec (Using Actual Pipe Body Shelf Energy)	S_a/S_f Mod Ln/Sec	Raju/Newman (Using 4 ft lb Shelf Energy)	S_a/S_f Raju/ Newman
31	94.1	100.1	0.94	43.5	2.16
32	94.3	108.7	0.87	46.2	2.04
33	94.9	100.6	0.94	42.5	2.24
34	95.8	120.8	0.79	46.4	2.07
35	95.9	111.9	0.86	73.9	1.30
36	96.1	100.3	0.96	49.0	1.96
37	97.3	76.9	1.26	35.0	2.78
38	98.0	92.1	1.06	33.1	2.96
39	100.7	77.2	1.30	43.8	2.30
40	102.2	109.8	0.93	86.5	1.18
41	103.2	71.6	1.44	22.6	4.56
42	112.5	105.6	1.07	33.9	3.32
43	112.5	96.4	1.17	38.2	2.95
44	112.6	96.4	1.17	38.2	2.95
45	113.5	122.3	0.93	91.1	1.25
46	115.6	74.4	1.55	39.5	2.92
47	116.1	98.4	1.24	48.8	2.50
48	117.1	89.9	1.30	36.8	3.18
49	118.7	65.6	1.81	28.4	4.18
50	120.2	76.2	1.58	34.3	3.50
51	126.4	102.9	1.23	50.6	2.50
52	126.4	66.6	1.90	25.3	5.00
53	127.1	114.0	1.07	80.2	1.52
54	132.5	72.2	1.84	26.4	5.01
55	135.6	80.0	1.69	29.1	4.66
56	135.6	86.1	1.58	37.6	3.61
57	135.6	81.9	1.66	36.8	3.68
58	138.7	74.5	1.86	34.3	4.04
59	140.2	99.7	1.41	30.5	4.60

As was the case with cold weld defects, the predicted failure stresses for the hook crack defects appear to have no correlation to the actual failure stresses. However, the S_a/S_f levels for the Raju/Newman predictions, except for one value of 0.99, are all greater than 1.0 indicating that they are conservative predictions.

There are three possible reasons for the lack of correlation. One is that the actual effective toughnesses of the regions near the bondline where hook cracks exist vary, and only by coincidence would the value happen to be either the same as the pipe body toughness or the arbitrarily chosen value represented by a Charpy energy of 4 ft lb. The second factor in the lack of correlation could be the fact that the shapes assumed for model analyses do not always reflect the actual shapes of the defects. The third possible reason is that ductile tearing that may be induced at a hook crack as the result of applied stress may cause a fracture of the bondline of the seam. An example of such an event (Hook Crack Failure Number 1) is shown in Figure 4.

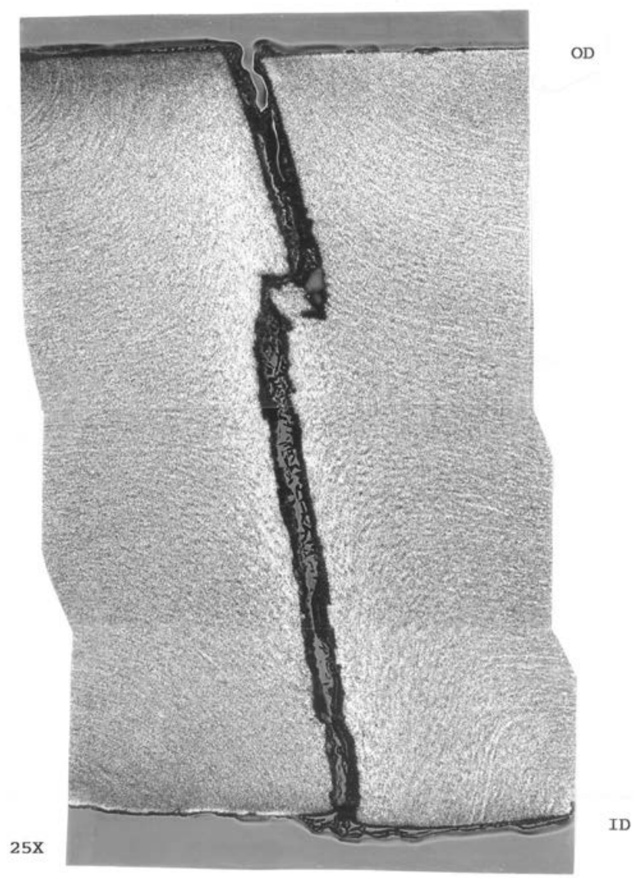

Figure 4. An Example of Fracture at a Hook Crack Failure Origin Jumping into the Bondline of the Seam

The significance of this phenomenon is believed to be the likelihood that such a failure can occur as a large pressure reversal when a sudden jump from a tearing crack in the heat-affected base metal to the bondline occurs. As discussed in Reference 1, a similar jump from a ductile tear at a hook crack to a bondline fracture is believed to have caused the failure of the Dixie Pipeline near Carmichael, MS in 2007.

Comparisons of the actual failure stresses to the predicted failure stresses for the 59 hook cracks are illustrated in Figure 5 and Figure 6. The sloping lines represent perfect agreement between actual and predicted stresses. The dashed vertical lines represent potential acceptance limits based on a predicted failure stress of 100% of SMYS.

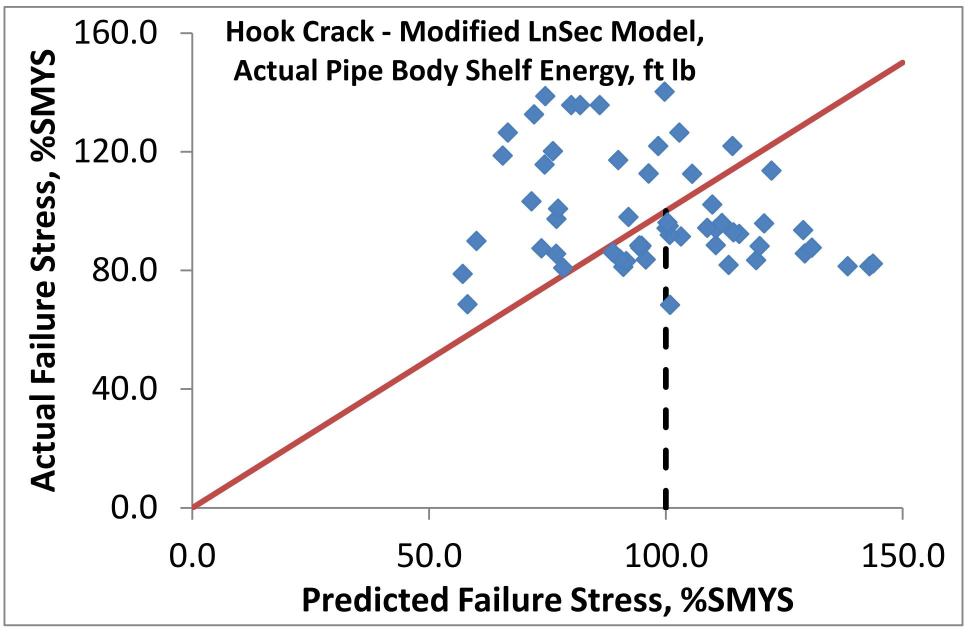

Figure 5. Comparisons of Actual to Predicted Failure Stresses for Hook Crack Anomalies Using the Modified LnSec Equation with the Actual Pipe Body Charpy Energy

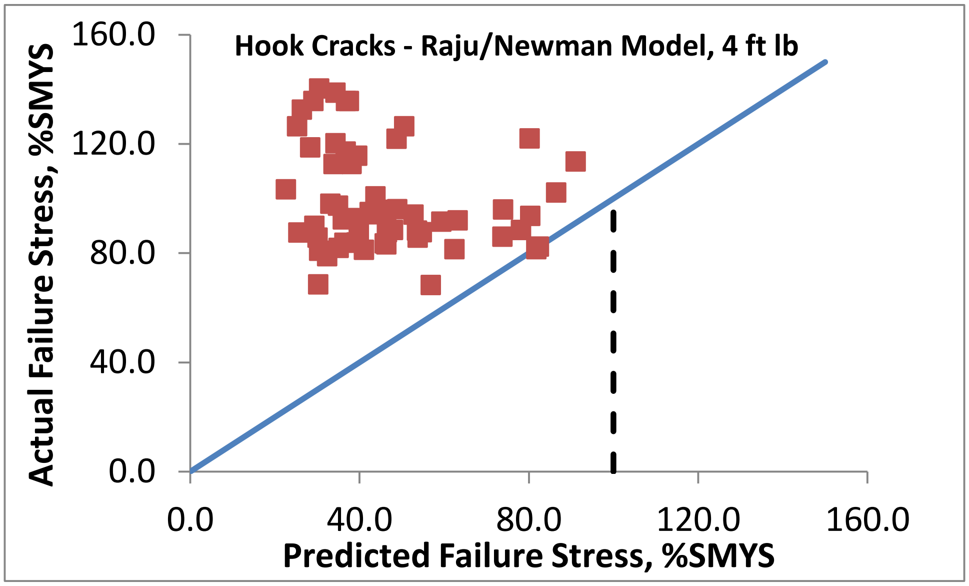

Figure 6. Comparisons of Actual to Predicted Failure Stresses for Hook Crack Anomalies Using the Raju/Newman Equation with a Charpy Energy of 4 ft lb

Very few of these comparisons resulted in agreement between the actual and the predicted failure stresses for the Modified LnSec equation using base metal toughness, most likely because the effective toughness in the vicinity of each hook crack was not the same as that of the base metal toughness. However, over-predictions in conjunction with the use of the Modified LnSec equation occurred less frequently for hook cracks than for cold welds. In 27 of 59 cases the model under-predicted the actual failure stress. In 12 additional cases the model gave predictions that were on the low side of but within 10 % of the actual failure stresses. The likely reason for the improved agreement in the case of hook cracks is that hook cracks do not lie on the bondline. As a result, the effective toughness of the material in which a hook crack resides is likely to be much higher than that of the bondline. These comparisons suggest that a ductile fracture initiation model could be used to reliably predict failure stresses for some hook cracks. However, 20 of predictions using the Modified LnSec equation over-estimated the actual failure stresses of the hook cracks by more than 10%. In contrast, it is seen that all except one of the predictions using the Raju/Newman equation with a Charpy energy of 4 ft lb are conservative (one of the S_a/S_f ratios was 0.99).

For the 20 cases where the Modified LnSec equation over-predicted the failure stresses by more than 10 percent (S_a/S_f ratios of less than 0.9), a follow-up analysis was made to see why the predictions were so poor. It was found that 9 of the 20 cases involved the fracture jumping from the hook crack to the bondline, 3 involved adjacent interacting hook cracks or planes of weakness (partly-bonded hook cracks), 3 involved brittle fracture of the base metal, 3 involved cases for which no evidence was available, and 2 were cases which cannot be explained on the basis of the photographs available.

As was shown for the cold welds discussed previously, the use a conservative, brittle fracture initiation model is likely to result in more hook crack anomalies not passing an acceptance limit than would be the case with a ductile fracture model. Consider the vertical dashed lines on Figure 5 and Figure 6 located at 100% of SMYS on the “Predicted Failure Stress” axis. If it is decided that all anomalies with predicted failure stress levels below 100% of SMYS must be excavated and examined, only 29 of the 59 anomalies would be excavated based on the Modified LnSec equation. In contrast, by this criterion all 59 anomalies would be excavated based on the Raju/Newman equation. As indicated in Table 5 and Table 6, the actual failure stress levels of 38 of the 59 anomalies were less than 100% of SMYS. One can also see from Table 5 that one of the anomalies that would not have been excavated based on the Modified LnSec equation had an actual failure stress less than 80% of SMYS. On the other hand, the use of the Raju/Newman model would have resulted in excavations of 21 anomalies that had actual failure stresses greater than 100% of SMYS. In the case of these 59 hook cracks, it would appear that the conservative approach of using a brittle fracture model gives greater assurance of pipeline integrity but at a price of making some unnecessary excavations.

Conclusions Regarding Predicting Failure Stress Levels for Hook Crack Anomalies

- Ductile fracture initiation models such as the Modified LnSec equation, PAFFC, or Corlas™ probably can be used to predict failure stress levels of hook crack anomalies that appear on a list of hook crack anomalies detected and sized by ILI if the effective toughness is equivalent to a Charpy upper-shelf energy of at least 15 ft lb. However, when the effective toughness is not known or when the possibility of a fracture jumping into a brittle bondline material exists, these models should not be used.
- The Raju/Newman equation can be used to predict conservative failure stress levels of hook crack anomalies detected and sized by ILI. A value of toughness corresponding to 4 ft lb of Charpy energy (equal to a fracture toughness of 22.4 $ksi\sqrt{inch}$ based on Equation 2) would seem to be an appropriate value to use to assure a conservative level of predicted failure stress.
- Using the more-conservative Raju/Newman model likely will result in a pipeline operator having to do more excavations of ILI-discovered anomalies. While the increased conservatism appears to be justified by some of the cases, it would have resulted in excavations of 21 hook cracks that probably did not need to be excavated based on their actual failure stress levels.

- As Leis has pointed out in Appendix A, a conservative approach is not appropriate for predicting the remaining lives of anomalies that could have survived a particular level of hydrostatic test stress. The appropriate approach for predicting the remaining lives will be presented in the Subtask 2.5 report.
- The K_r portion of a FAD calculation based on an API 579-2/ASME FFS-1 – Fitness-for-Service, Level II calculation could be used in place of the Raju/Newman calculation because the two calculations give virtually the same answers if the same K_c value is used.

Predictions of Failure Stress for Selective Seam Weld Corrosion Defects

Presented in Table 7 are 12 cases involving selective seam weld corrosion defects that failed. The table lists the attributes of the pipeline material, the failure stress as a percent of SMYS, the key pipe body properties, and the dimensions of the anomalies that caused the failures. All of these cases involve either LF-ERW or DC-ERW pipe. Selective seam weld corrosion (SSWC) has been known to occur in flash-welded seams and HF-ERW seams. However, no case of SSWC in a flash-welded seam was contained in the database, and the flaw dimensions for SSWC ruptures in the HF-ERW pipe were unavailable. For cross reference with the Subtask 1.4 report, the Case Number as used in that report is included as well.

Table 7. Attributes of ERW Materials and Selective Seam Weld Corrosion Anomalies that Caused Failures (The yellow highlighted items represent reasonable assumed values where the actual data was not provided.)

SSWC Failure Number	Case Number (from Reference 1)	Diameter, inch	Wall Thickness, inch	Grade	SMYS	Seam Type	Failure Pressure, %SMYS	Pipe Body Properties			Anomaly Dimensions	
								Actual Yield Strength, psi	Actual Ultimate Strength, psi	Charpy Upper Shelf Energy, ft lb (full-	Length, inches	Depth, inch
1	1	10.75	0.279	X46	46,000	ERW - LF	28.5	57,000	74,500	21	5.00	0.165
2	4	12.75	0.250	X52	52,000	ERW - LF	61.6	60,000	76,000	23	6.50	0.165
3	9	8.625	0.250	X42	42,000	ERW - LF	41.1	47,600	63,500	25	1.00	0.175
4	12	18	0.250	X42	42,000	ERW - DC	31.2	52,500	80,500	25	3.30	0.075
5	14	12.75	0.250	X46	46,000	ERW - LF	86.9	56,000	76,500	37	2.00	0.060
6	15	16	0.375	Grade B	35,000	ERW - LF	7.3	51,500	71,000	20	5.40	0.242
7	16	12.75	0.250	Grade B	35,000	ERW - LF	81.2	57,000	77,500	26	3.00	0.220
8	17	8.625	0.203	X42	42,000	ERW - LF	92.3	55,000	74,500	56	1.00	0.183
9	18	8.625	0.203	X42	42,000	ERW - LF	79.7	63,500	81,500	31	3.75	0.100
10	19	10.75	0.219	X46	46,000	ERW - LF	74.7	62,000	73,500	41	3.00	0.110
11	21	12.75	0.312	-	42,000	ERW - LF	31.6	63,000	78,000	18	6.00	0.172
12	22	8.625	0.219	X46	46,000	ERW - LF	47.8	52,000	66,400	16	0.40	0.150

For each selective seam weld corrosion anomaly, two calculations of predicted failure stress levels were made, one using the Modified LnSec equation with the Charpy energy measured for the pipe body material, and one using the Raju/Newman equation with the Charpy energy fixed at 0.4 ft lb. As will become apparent the Raju/Newman equation provides lower bound predictions for the selective seam weld corrosion defects when used with a toughness level corresponding to a Charpy energy of 0.4 ft lb. Note that the latter is only one tenth the level used in conjunction with similar comparisons for cold welds and hook cracks.

The predicted failure stress levels for the 12 selective seam weld corrosion anomalies are presented in Table 8 along with the actual failure stress levels. The ratios, S_a/S_f, (actual to predicted failure stress) for each model are also given in the column next to the failure stress predicted by each model.

Table 8. Failure Stress Levels for Selective Seam Weld Corrosion Anomalies Predicted by Both Methods Compared to Actual Failure Stress Levels

SSWC Failure No.	Actual Failure Stress, %SMYS	Predicted Failure Stress, % SMYS			
		Modified LnSec (Using Actual Pipe Body Shelf Energy)	S_a/S_f Mod. LnSec	Raju/Newman (Using 0.4 ft lb Shelf Energy)	S_a/S_f Raju/ Newman
1	28.5	80.3	0.35	6.0	4.73
2	61.6	58.0	1.06	4.2	14.81
3	41.1	115.8	0.35	10.9	3.76
4	31.2	132.6	0.24	16.3	1.91
5	86.9	135.8	0.64	18.2	4.78
6	7.3	100.5	0.07	6.7	1.08
7	81.2	58.7	1.38	6.9	11.85
8	92.3	82.8	1.11	10.2	9.06
9	79.7	116.7	0.68	9.8	8.10
10	74.7	114.6	0.65	9.2	8.11
11	31.6	93.2	0.34	6.7	4.70
12	47.8	130.3	0.37	16.8	2.84

Comparisons of the predicted failure stresses to actual failure stresses for the two calculation methods are shown in Figure 7 and Figure 8. The predicted failure stresses of neither model seem to be correlated with the actual failure stresses. As stated before the lack knowledge of the actual toughness and the fact that the shapes assumed for model analyses do not always reflect the actual shapes of the defects, contribute to the lack of correlation. However, the Modified LnSec equation predictions greatly over-estimated all but three of the actual failure stress levels, whereas the Raju/Newman calculations provides lower-bound estimates of actual failure stresses.

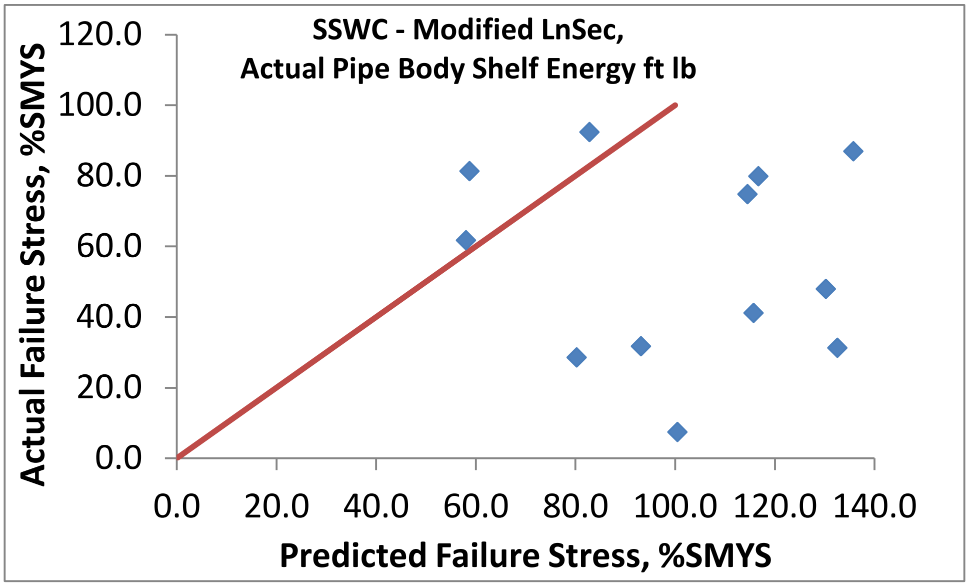

Figure 7. Comparisons of Actual to Predicted Failure Stresses for Selective Seam Weld Corrosion Anomalies Using the Modified LnSec Equation with the Actual Pipe Body Charpy Energy

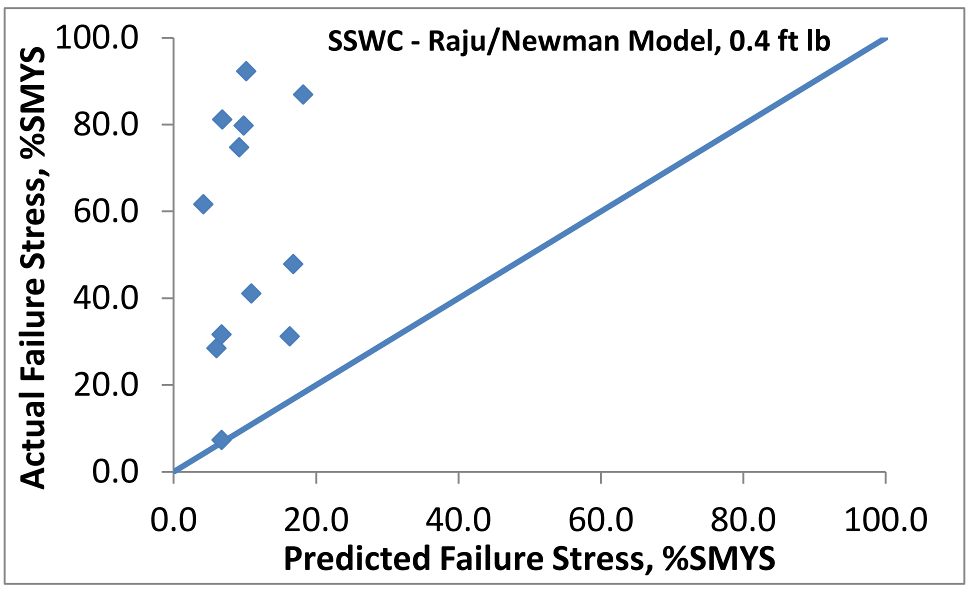

Figure 8. Comparisons of Actual to Predicted Failure Stresses for Selective Seam Weld Corrosion Anomalies Using the Raju/Newman Equation with a Charpy Energy of 0.4 ft lb

In two of the three cases where the actual failure stress exceeded the failure stress calculated via the Modified LnSec equation (SSWC Failure Numbers 7 and 8), the anomalies were quite deep (88 and 90 percent through the wall). It is likely that the small remaining ligament in each case failed in a ductile manner. In such a case it is not surprising to find that a ductile fracture model gave a reasonable prediction of the actual failure stress. In the remaining case where the actual failure stress exceeded the failure stresses calculated via the Modified LnSec equation (SSWC Failure Number 2), the anomaly had a blunt shape as shown in Figure 9. Such a shape would tend to force the failure to initiate in a ductile manner. The crack path shown in Figure 9 is suggestive of ductile tearing. For this case, the ratio of the actual failure stress to the failure stress predicted by the Modified LnSec equation is 1.06, showing that the model performed satisfactorily for this case of apparently ductile fracture initiation.

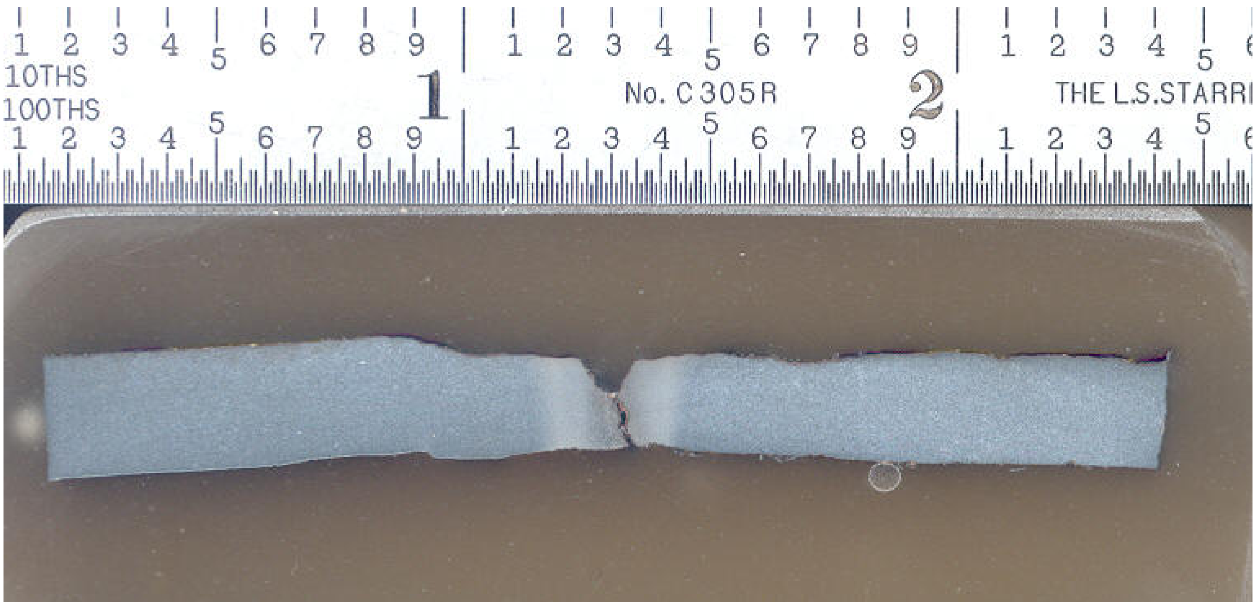

Figure 9. Appearance of the Selective Seam Weld Corrosion Associated with SSWC Failure Number 2

In contrast, in the nine cases where the Modified LnSec equation greatly over-estimated the failure stresses, the anomalies tended have sharp tips and the behavior of the remaining ligament upon failure was extremely brittle. An example, SSWC Failure Number 6, is shown in Figure 10. The overall length of the defect was 5.4 inches and it penetrated 65% of the wall thickness at the deepest point. The predicted failure stress for this defect using the Modified LnSec equation with the pipe body Charpy energy of 36 ft lb is 100.5 % of SMYS. This failure occurred at the lowest stress level of the 12 cases, 7.3% of SMYS, and the material exhibited the least toughness of any of those involved in the 12 cases. The fracture did not propagate through the entire seam because of the low stress level. As a result, another area of selective seam weld corrosion in the same pipe remained intact. The selective seam weld corrosion in that region was over 12 inches long and penetrated 87% of the wall thickness at the deepest point. That segment was later pressurized to failure in a burst test, and even though it was a larger defect than the one that caused the in-service failure, it failed at a stress level of 21% of SMYS. These two failures in the same piece of pipe show that the toughness can vary significantly along an ERW seam.

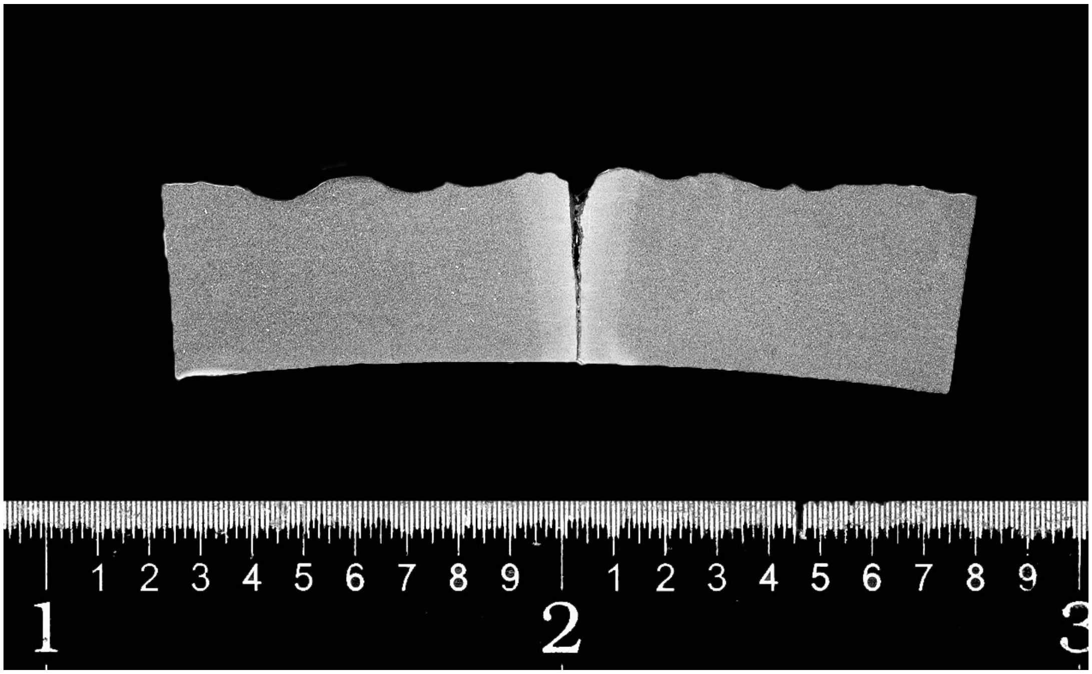

Figure 10. Appearance of the Selective Seam Weld Corrosion Associated with SSWC Failure Number 6

For all 12 of these SSWC anomalies the Raju/Newman equation provided a lower-bound prediction of the failure stress levels on the basis of the assumed toughness level corresponding to 0.4 ft lb (equal to a fracture toughness of 5.2 $ksi\sqrt{inch}$ based on Equation 2). In most of the cases this assumed low level of toughness resulted in significant under-estimates of the actual failure pressure, and that might have led to the excavation and examination of anomalies that would not necessarily have impaired the safety of the pipeline. However, SSWC anomalies are likely to grow worse with time. Therefore, it is not necessarily a bad thing if they are excavated and examined.

Conclusions Regarding Predicting Failure Stress Levels for Selective Seam Weld Corrosion Anomalies

- Ductile fracture initiation models such as the Modified LnSec equation, PAFFC, or Corlas™ should not be used to predict failure stress levels of selective seam weld corrosion anomalies in LF-ERW, DC-ERW, or flash-welded seams that appear on a list of such anomalies detected and sized by ILI.
- The Raju/Newman equation can be used to predict conservative failure stress levels of selective seam weld corrosion anomalies detected and sized by ILI. A value of toughness corresponding to 0.4 ft lb of Charpy energy (equal to a fracture toughness of 5.2

$ksi\sqrt{inch}$ based on Equation 2) would seem to be an appropriate value to use to assure a conservative level of predicted failure stress.

- The toughness of an ERW seam within a single piece of pipe can vary significantly from point to point along the seam.
- Using the more-conservative (and more appropriate) Raju/Newman model likely will result in a pipeline operator having to do more excavations of ILI-discovered anomalies.
- As Leis has pointed out in Appendix A, a conservative approach is not appropriate for predicting the remaining lives of anomalies that could have survived a particular level of hydrostatic test stress. The appropriate approach for predicting the remaining lives will be presented in the Subtask 2.5 report.
- The K_r portion of a FAD calculation based on an API 579-2/ASME FFS-1 – Fitness-for-Service, Level II calculation could be used in place of the Raju/Newman calculation because the two calculations give virtually the same answers if the same K_c value is used.

Predictions of Failure Stress for Defects Enlarged by Fatigue

Presented in Table 9 are 32 cases involving fatigue-enlarged defects that failed. The table lists the attributes of the pipeline material, the failure stress as a percent of SMYS, the key pipe body properties, and the dimensions of the anomalies that caused the failures. For cross reference with the Subtask 1.4 report, the Case Number as used in that report is included as well. These 32 cases were among 37 cases examined in Reference 1. Five of the 37 cases were not included herein because the dimensions of the anomalies in those 5 cases were not available. Also, in a change from Reference 1 the length of Fatigue Failure Number 1 was changed from 2.4 inches to 4 inches because a review of a picture of the fracture surface indicated the longer length to be the correct length.

Table 9. Attributes of ERW Materials and Fatigue-Enlarged Anomalies that Caused Failures (The yellow highlighted items represent reasonable assumed values where the actual data was not provided.)

Fatigue Failure Number	Case Number (from Reference 1)	Diameter, inch	Wall Thickness, inch	Grade	SMYS	Seam Type	Failure Pressure, %SMYS	Pipe Body Properties: Actual Yield Strength, psi	Pipe Body Properties: Actual Ultimate Strength, psi	Pipe Body Properties: Charpy Upper Shelf Energy, ft lb (full-	Anomaly Dimensions: Length, inches	Anomaly Dimensions: Depth, inch
1	2	12.75	0.219	X52	52,000	ERW - LF	66.9	67,000	93,000	26	7.00	0.198
2	4	10.75	0.25	X46	46,000	Flash-weld	95.8	54,000	69,000	22	2.33	0.180
3	5	10.75	0.25	X46	46,000	Flash-weld	79.8	62,000	81,500	29	7.00	0.176
4	6	10.75	0.307	X46	46,000	ERW - LF	81.2	54,500	75,500	27	4.20	0.230
5	7	12.75	0.25	X45	45,000	Flash-weld	61.7	60,500	76,000	36	4.00	0.198
6	8	8.625	0.188	X52	52,000	ERW - LF	69.7	50,000	73,500	18	6.50	0.132
7	9	10.75	0.219	X52	52,000	ERW - LF	81.8	66,500	93,500	57	5.00	0.125
8	10	6.625	0.125	X60	60,000	ERW - HF	93.7	68,500	75,500	30	6.00	0.070
9	11	12.75	0.203	X52	52,000	ERW - LF	59.8	53,000	68,000	49	4.00	0.163
10	12	16	0.25	X52	52,000	ERW - DC	81.6	55,000	73,000	21	2.50	0.175
11	13	16	0.25	X52	52,000	ERW - DC	81.8	55,000	67,500	30	9.00	0.102
12	14	20	0.312	X52	52,000	Flash-weld	55.3	57,000	83,000	25	3.50	0.248
13	15	12.75	0.25	X46	46,000	ERW - LF	97.0	56,000	73,500	28	4.00	0.125
14	16	12.75	0.25	X46	46,000	ERW - LF	96.5	54,500	70,000	29	4.30	0.144
15	17	12.75	0.25	X46	46,000	ERW - LF	94.7	53,500	71,500	30	2.00	0.195
16	19	22	0.312	X46	46,000	ERW - DC	78.0	52,000	75,000	25	3.60	0.173
17	20	8.625	0.203	Grade B	35,000	Flash-weld	69.8	49,600	64,000	34	1.44	0.179
18	21	10.75	0.219	X52	52,000	ERW - LF	81.6	65,000	94,500	45	14.70	0.088
19	22	10.75	0.219	X52	52,000	ERW - LF	87.2	67,500	93,000	43	7.00	0.076
20	23	26	0.281	X52	52,000	Flash-weld	87.8	53,500	76,000	30	10.00	0.141
21	26	20	0.219	X52	52,000	ERW - HF	54.3	59,500	76,500	32	4.50	0.208
22	27	18	0.219	X52	52,000	ERW - DC	60.6	80,000	82,000	44	8.50	0.188
23	28	26	0.281	X52	52,000	Flash-weld	64.5	60,500	86,800	41	5.25	0.197
24	29	8.625	0.188	X46	46,000	ERW - LF	67.8	54,000	78,000	36	12.00	0.121
25	30	24	0.328	X70	70,000	ERW - HF	69.6	77,250	90,250	116	36.80	0.200
26	31	20	0.312	X52	52,000	Flash-weld	115.6	52,000		25	4.50	0.176
27	32	20	0.312	X52	52,000	Flash-weld	95.5	52,000		25	12.00	0.250
28	33	20	0.312	X52	52,000	Flash-weld	107.9	52,000		25	19.50	0.218
29	34	20	0.312	X52	52,000	Flash-weld	120.2	52,000		25	12.00	0.189
30	35	20	0.312	X52	52,000	Flash-weld	55.3	52,000		25	132.00	0.162
31	36	26	0.281	X52	52,000	Flash-weld	100.0	73,000	81,000	25	2.00	0.272
32	37	20	0.230	X52	52,000	ERW - DC	70.8	57,000	74,000	36	3.4	0.198

It is recalled from Reference 1 that 28 of the 37 fatigue failures initiated at hook cracks, 6 initiated at mismatched plate edges, and 3 were attributed to the following: a damaged edge, an “ID feature”, and a cold weld in HF-ERW pipe. Except for the case of the cold weld (no picture of which was available for analysis), all of the fatigue cracks appeared to have propagated in base metal and not in the bondline. A typical example is shown in Figure 11. In this case the fatigue initiated at an ID-surface-connected hook crack and propagated in heat-affected base metal by fatigue to a depth of about 80 percent of the wall thickness. The remaining ligament failed by ductile tearing.

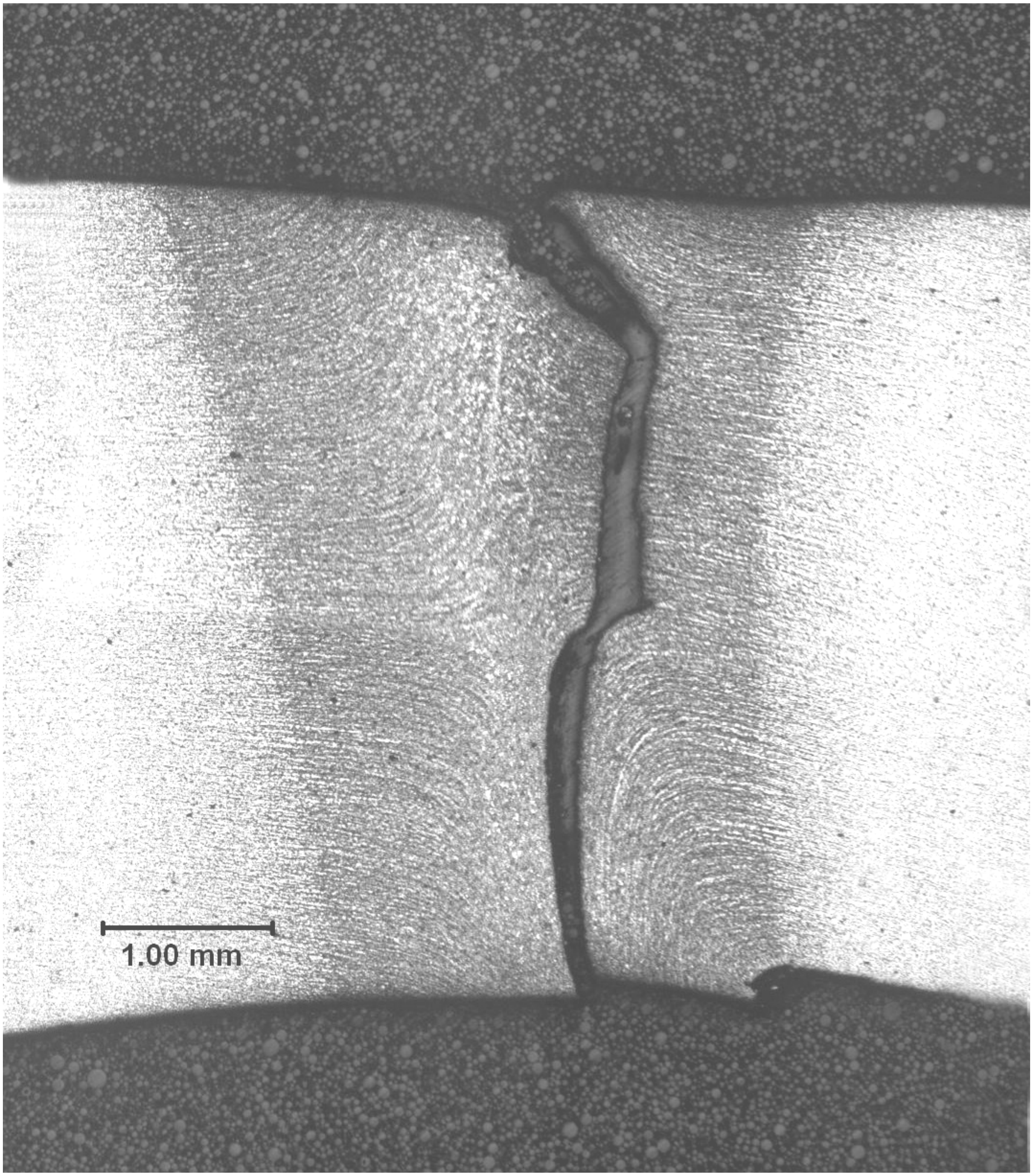

Figure 11. Example of Fatigue-Enlargement of an ID-Surface-Connected Hook Crack (Fatigue Failure Number 9)

For each fatigue failure anomaly, two calculations of predicted failure stress levels were made, one using the Modified LnSec equation with the Charpy energy measured for the pipe body material, and one using the Raju/Newman equation with the Charpy energy fixed at 8 ft lb. As will become apparent the Raju/Newman equation provides lower bound predictions for the fatigue-enlarged defects when used with a toughness level corresponding to a Charpy energy of 8 ft lb. The predicted failure stress levels for 32 fatigue failure anomalies are presented in Table 10 along with the actual failure stress levels. The ratios, S_a/S_f, (actual to predicted failure stress) for each model are also given in the column next to the failure stress predicted by each model.

Table 10. Failure Stress Levels for Fatigue-Enlarged Anomalies Predicted by Both Methods Compared to Actual Failure Stress Levels

Fatigue Failure No.	Actual Failure Stress, %SMYS	Predicted Failure Stress, % SMYS			
		Modified LnSec (Using Actual Pipe Body Shelf Energy)	S_a/S_f Mod. LnSec	Raju/Newman (Using 8 ft lb Shelf Energy)	S_a/S_f Raju/ Newman
1	66.9	19.1	3.51	14.6	4.57
2	95.8	84.7	1.13	45.6	2.10
3	79.8	58.1	1.37	26.6	3.00
4	81.2	61.3	1.33	32.2	2.52
5	61.7	60.6	1.02	31.9	1.93
6	69.7	41.0	1.70	24.8	2.81
7	81.8	84.7	0.97	38.9	2.10
8	93.7	63.1	1.48	38.1	2.46
9	59.8	42.6	1.40	26.4	2.26
10	81.6	83.7	0.97	40.8	2.00
11	81.8	81.2	1.01	55.9	1.46
12	55.3	65.7	0.84	31.0	1.78
13	97.0	100.9	0.96	63.2	1.54
14	96.5	87.2	1.11	44.9	2.15
15	94.7	84.4	1.12	46.6	2.03
16	78.0	115.8	0.67	68.2	1.14
17	69.8	74.7	0.93	66.8	1.04
18	81.6	83.9	0.97	57.4	1.42
19	87.2	107.2	0.81	73.6	1.18
20	87.8	71.4	1.23	39.0	2.25
21	54.3	15.5	3.50	20.1	2.70
22	60.6	31.9	1.90	14.5	4.19
23	64.5	73.0	0.88	28.3	2.28
24	67.8	52.5	1.29	28.0	2.43
25	69.6	43.8	1.59	14.7	4.73
26	115.6	82.6	1.40	39.2	2.95
27	95.5	27.9	3.43	14.1	6.78
28	107.9	32.5	3.32	16.1	6.71
29	120.2	51.2	2.35	25.3	4.74
30	55.3	38.3	1.44	27.6	2.00
31	100.0	42.3	2.37	38.3	2.61
32	70.8	46.4	1.53	28.5	2.48

Comparisons of the predicted failure stresses to actual failure stresses for the two calculation methods are shown in Figure 12 and Figure 13. The predicted failure stresses of neither model seem to be correlated with the actual failure stresses. As stated before the lack knowledge of the actual toughness and the fact that the shapes assumed for model analyses do not always reflect the actual shapes of the defects, contribute to the lack of correlation. However, the Modified LnSec equation predictions conservatively estimated many of the actual failure stress levels, and the Raju/Newman calculations provided lower-bound estimates for all of actual failure stresses when a toughness corresponding to a Charpy energy of 8 ft lb was used.

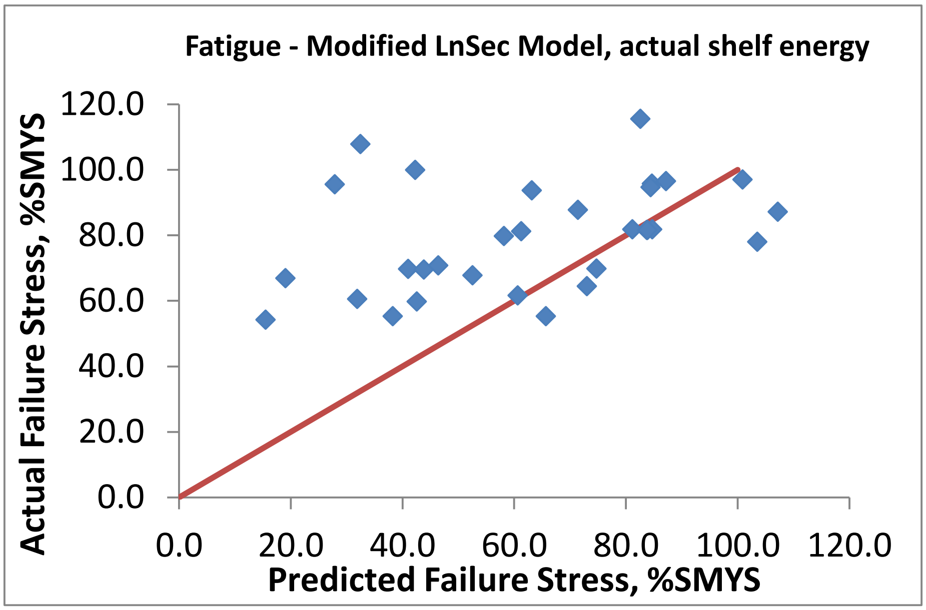

Figure 12. Comparisons of Actual to Predicted Failure Stresses for Fatigue-Enlarged Anomalies Using the Modified LnSec Equation with the Actual Pipe Body Charpy Energy

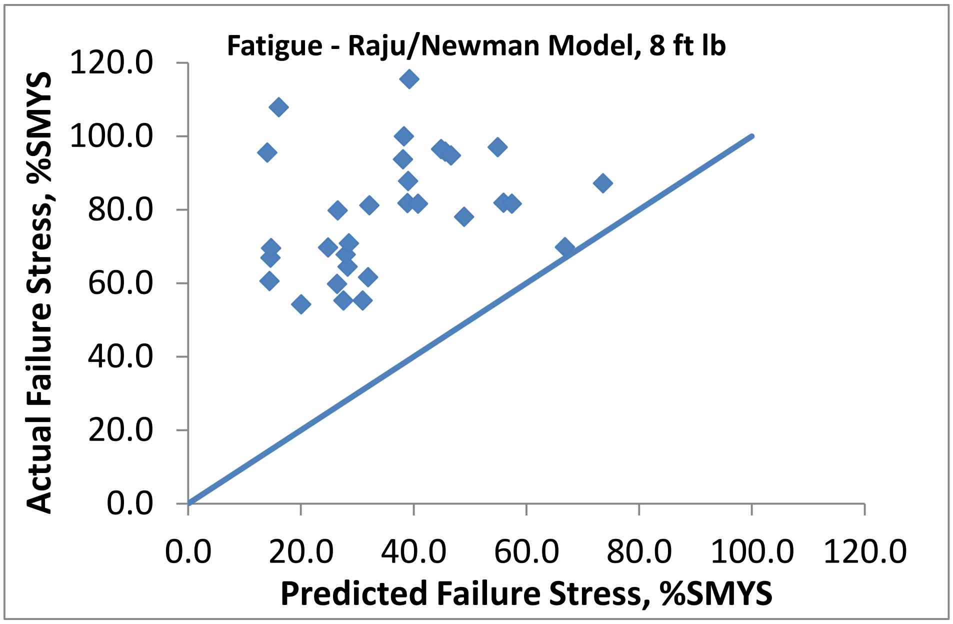

Figure 13. Comparisons of Actual to Predicted Failure Stresses for Fatigue-Enlarged Anomalies Using the Raju/Newman Equation with a Charpy Energy of 8 ft lb

The failure stresses were calculated again via the Modified LnSec equation using a fixed Charpy energy level of 15 ft lb. The results are presented in Table 11, and the comparisons of predicted to actual failure stresses are shown in Figure 14.

Table 11. Failure Stress Levels for Fatigue-Enlarged Anomalies Predicted by the Modified LnSec Method Using a Charpy Energy of 15 ft lb Compared to Actual Failure Stress Levels

Fatigue Failure No.	Actual Failure Stress, %SMYS	Modified LnSec (Using 15 ft lb Shelf Energy)	S_a/S_f Mod. LnSec
1	66.9	16.4	4.07
2	95.8	84.2	1.14
3	79.8	50.3	1.59
4	81.2	58.5	1.39
5	61.7	56.5	1.09
6	69.7	39.7	1.76
7	81.8	73.3	1.12
8	93.7	55.2	1.70
9	59.8	40.8	1.46
10	81.6	83.0	0.98
11	81.8	73.4	1.11
12	55.3	63.4	0.87
13	97.0	96.3	1.01
14	96.5	82.8	1.17
15	94.7	84.2	1.13
16	78.0	104.8	0.74
17	69.8	74.7	0.93
18	81.6	73.2	1.11
19	87.2	94.8	0.92
20	87.8	62.9	1.40
21	54.3	14.3	3.79
22	60.6	22.9	2.65
23	64.5	64.7	1.00
24	67.8	42.8	1.58
25	69.6	32.3	2.15
26	115.6	79.1	1.46
27	95.5	24.0	3.98
28	107.9	28.3	3.82
29	120.2	45.4	2.65
30	55.3	37.7	1.47
31	100.0	41.3	2.42
32	70.8	44.8	1.58

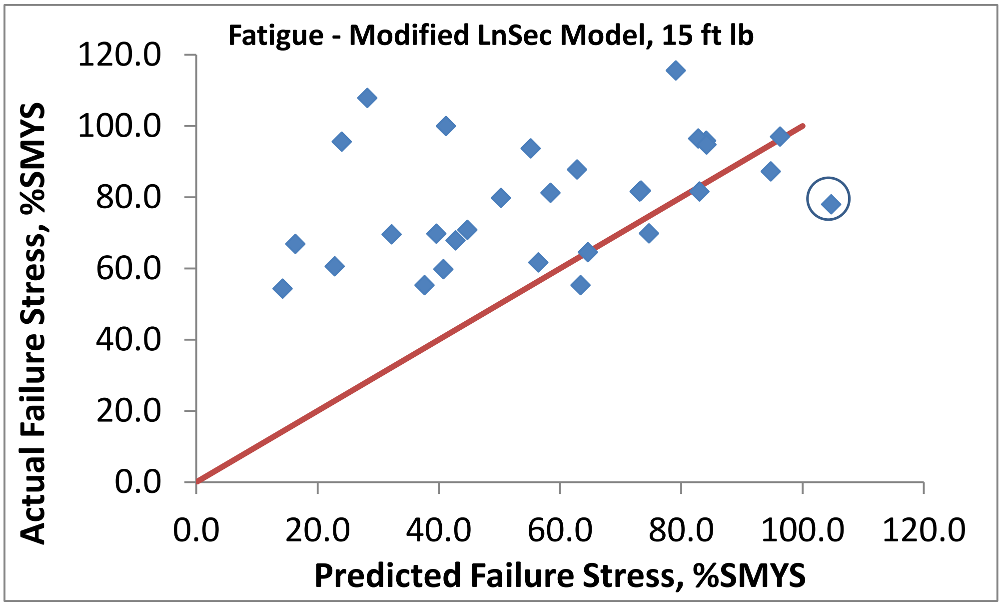

Figure 14. Comparisons of Actual to Predicted Failure Stresses for Fatigue-Enlarged Anomalies Using the Modified LnSec Equation with a Charpy Energy of 15 ft lb

It is seen in Figure 14 that all but five of the predicted failure stresses either agreed well with or gave conservative estimates of the actual failure stresses. Four of the remaining five gave predictions ranging from 87% to 98% of the actual failure stresses. The only case in which the agreement was not good (the encircled point in Figure 14) turned out to be one in which the failure appeared to have initiated as a brittle fracture. The fracture surface of this specimen is shown in Figure 15. It turns out that this failure occurred in an inadequately post-weld heat treated seam. The hardness levels in and around the seam ranged from 31 Rockwell C to 42 Rockwell C. Such a material likely has an un-tempered martensite microstructure. Brittle behavior of such a material is not unexpected. This Grade X46 material was made by Youngstown Sheet and Tube Company in 1949. During that timeframe excessively high hardness was a common problem for the heat-affected zones of Youngstown ERW pipe.

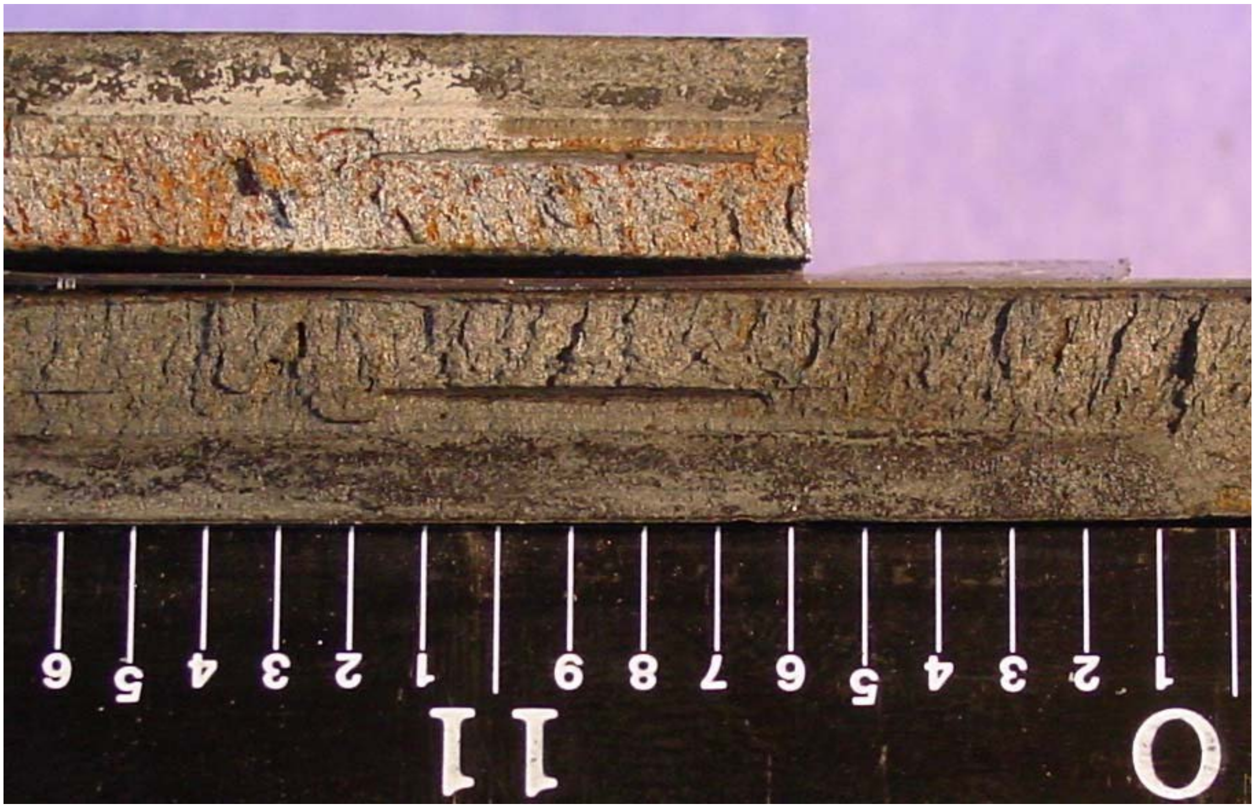

Figure 15. Fatigue Failure No. 16 Showing the Brittle Nature of the Failure of the Remaining Ligament

Conclusions Regarding Predicting Failure Stress Levels for Fatigue-Enlarged Anomalies

- Ductile fracture initiation models such as the Modified LnSec equation, PAFFC, or Corlas™ apparently can be used to predict failure stress levels of fatigue-enlarged anomalies that appear on a list of such anomalies detected and sized by ILI. When the Modified LnSec equation was used with a toughness corresponding to a Charpy energy of 15 ft lb, it gave acceptable estimates of the failure stress levels in all cases where the failure initiated in a ductile manner. The only case for which the Modified LnSec equation gave a significantly un-conservative prediction of the failure stress involved a unique case of brittle fracture in an excessively hard material.
- The Raju/Newman equation is probably not a suitable model to use for calculating failure stress levels for fatigue-enlarged anomalies near ERW seams because such flaws tend to fail in a ductile mode.

DISCUSSION

Overview of the Findings

Two models for predicting the failure stress levels of axial defects in pressurized pipe were examined in this study. One, the Modified LnSec equation, is an empirical model that has been shown to work well for predicting the failure stress levels of defects in conventional line pipe materials that behave in a ductile manner. The other, the Raju/Newman equation, is a variation of the classic fracture mechanics equation that is based on the concept of a crack failing in a brittle manner when the applied stress causes the stress intensity factor, K, to reach a critical value. The data presented herein show that both equations have their uses depending on the circumstances.

Of the four types of ERW seam defects considered herein, two types, cold welds and selective seam weld corrosion, reside in the bondlines of ERW seams. In the cases of LF-ERW, DC-ERW, and flash- welded pipe, the bondline regions tend to be prone to brittle fracture in the presence of a defect. For these types of defects, the data examined herein suggest that the Raju/Newman model is the best means of predicting a conservative value of failure stress. It was shown that the Raju/Newman equation predicted lower-bound values of the actual failure stresses for 21 cold weld defects when the critical stress intensity factor, K_c, was assumed to be 22.4 $ksi\sqrt{inch}$. According to the Charpy-to- K_c relationship used in this report (Equation 2), this level of fracture toughness corresponds to a Charpy energy of 4 ft lb, a value that is considerably lower than the level typically exhibited by the base metal of a conventional line pipe material. Similarly, it was shown that the Raju/Newman equation predicted lower-bound values of the actual failure stresses for 12 selective seam weld corrosion defects when the critical stress intensity factor, K_c, was assumed to be 5.2 $ksi\sqrt{inch}$. According to the Charpy-to- K_c relationship used in this report (Equation 2), this level of fracture toughness corresponds to a Charpy energy of 0.4 ft lb, a value that is extremely low compared to the level typically exhibited by the base metal of a conventional line pipe material.

The other two types of ERW seam defects considered herein, hook cracks and defects that fail after being enlarged by pressure-cycle-induced fatigue, tend to be located in the zone of heat-affected base metal near the bondlines of ERW seams. Even in LF-ERW, DC-ERW, and flash-welded materials, these zones tend to exhibit fracture behavior that is ductile as long as the fractures do not jump to the bondlines. For these types of defects the data examined herein suggest that, as long as the heat-affected material itself is not prone to exhibit brittle fracture and as long as the fracture does not jump into the bondline, the Modified LnSec equation tends to give reasonable predictions of the actual failure stress levels of the defects. The Modified LnSec equation when used with toughness levels corresponding to the Charpy upper shelf energy for the base metal gave lower-bound predictions of the actual failure stresses for 27 of the 59 hook cracks, and predictions within 90% of the actual failure stresses in an additional 12 cases. For the remaining 20 cases the Modified LnSec equation over-estimated the actual failure stresses by more than 10%. The primary reason for the over-estimates was brittle fracture behavior. In 9 of the 20 cases, the fractures jumped into the bondlines of the materials. For the remaining 11 cases, the reasons for the over-estimates were not always clear, although brittle fracture in the base metal or the presence of other interacting defects accounted for 6 of the 11 cases.

In 27 of the 32 cases of the defects enlarged by fatigue, failure stresses predicted via the Modified LnSec equation using a fixed value of 15 ft lb to represent toughness either agreed well with or were conservative estimates of the actual failure stresses. In 4 of the 32 cases the Modified LnSec equation used with 15 ft lb gave estimates of failure stresses that ranged from 87% to 98% of the actual failure stresses. In the one remaining case where the Modified LnSec equation used with 15 ft lb gave an estimated failure stress of only 74% of the actual failure stress, it was found that the failure had occurred in a brittle manner in an excessively hard heat-affected material.

The differences in failure behavior that are implied by the above comparisons can be seen graphically in terms of the sizes and failure stresses of the four types of defects associated with the observed failures. To represent the sizes in terms of only one parameter where size is normally given in two parameters, length and depth, one can use the relative area of the defect: length times the depth/wall thickness ratio. The relative sizes of the defects examined herein are displayed in Figure 16 and the failure stresses are displayed in Figure 17. Each of the four different types of defects, cold welds, hook cracks, selective seam weld corrosion, and fatigue is represented by a different symbol. The relative sizes of most of the hook cracks and the fatigue cracks are considerable larger than those of the cold welds and selective seam weld corrosion defects. At the same time the failure stresses of most of the hook cracks and fatigue cracks are in the same range as or higher than those of the cold welds and selective seam weld corrosion defects. This is indicative of the fact that, in most cases, the toughnesses associated with the failures of the hook cracks and fatigue cracks are significantly higher than those associated with failures of the bondline defects. The most plausible explanation is that most of the hook cracks and fatigue cracks failed in a ductile manner whereas most of the bondline defects failed in a brittle manner.

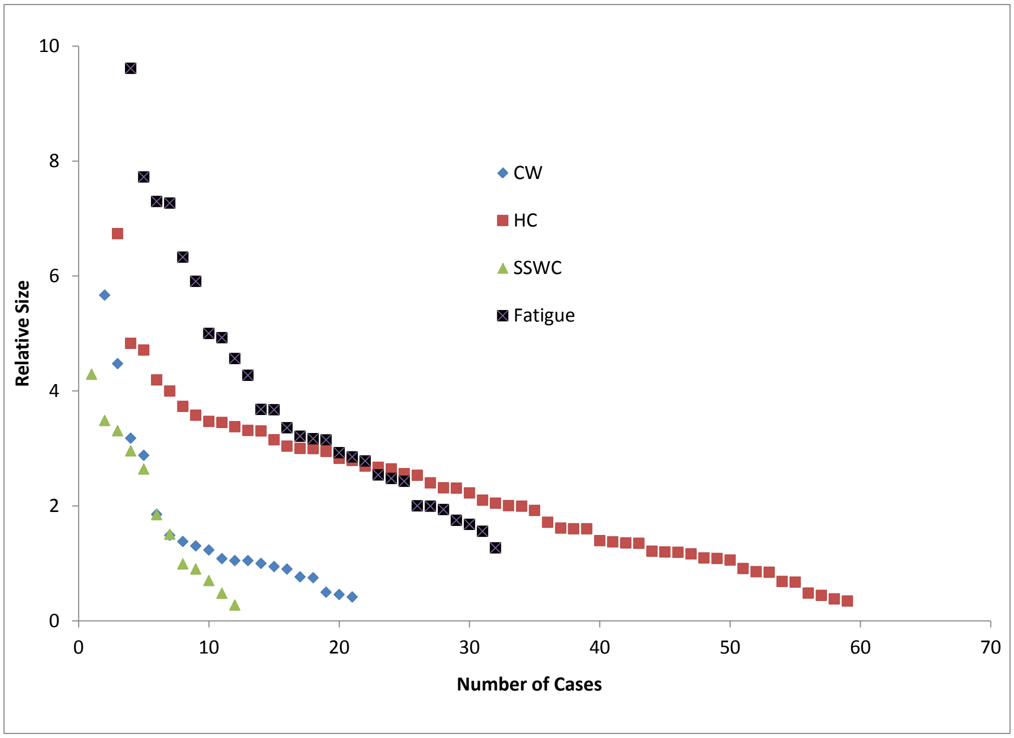

Figure 16. Relative Sizes of the Defects Compared by Type

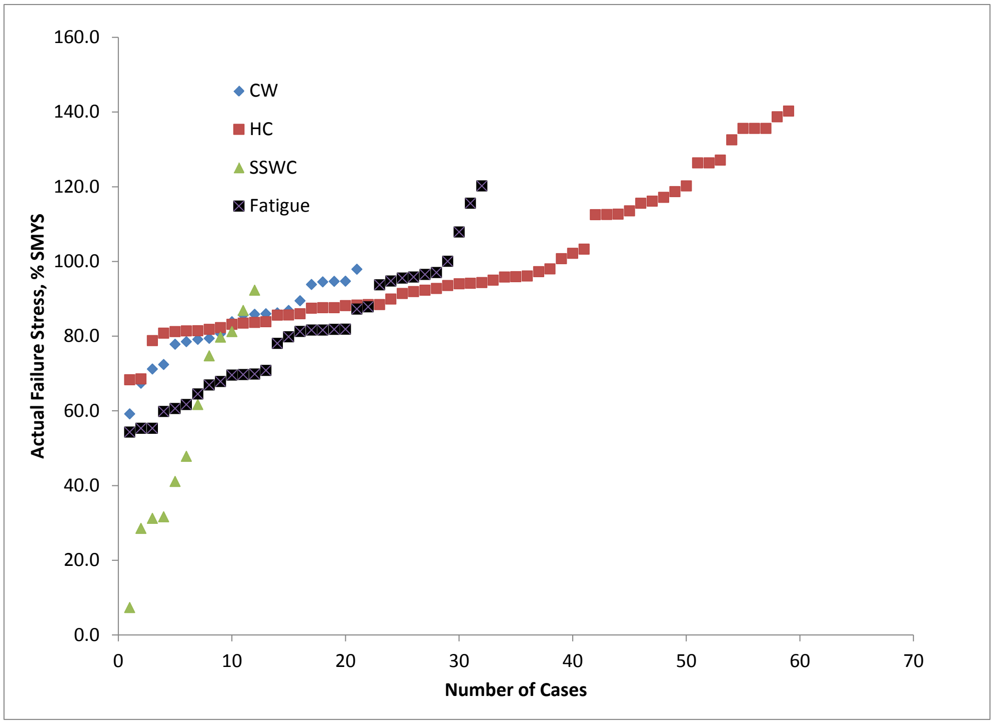

Figure 17. Failure Stresses of the Defects Compared by Type

Conclusions Regarding the Models Assessed Herein

The conclusions that arise from this study are as follows.

1. Defects in the bondlines of LF-ERW, DC-ERW, and flash-welded seams such as cold welds and selective seam weld corrosion tend to fail in a brittle manner. Therefore, it is inappropriate to use a ductile fracture model to predict their failure stresses. A more appropriate model would be one that is tailored to predicting brittle fracture initiation. The Raju/Newman equation was shown herein to predict lower-bound estimates of the actual failure stresses of bondline defects when used with an appropriate toughness level.

2. The Raju/Newman equation when used with a fracture toughness level of 22.4 $ksi\sqrt{inch}$ (corresponding to a Charpy energy of 4 ft lb) was found to give lower-bound estimates of the failure stresses of 21 cold weld defects.

3. The Raju/Newman equation when used with a fracture toughness level of 5.2 $ksi\sqrt{inch}$ corresponding to a Charpy energy of 0.4 ft lb) was found to give lower-bound estimates of the failure stresses of 12 selective seam weld corrosion defects.

4. Defects in the heat-affected base metal near LF-ERW, DC-ERW, and flash-welded seams such as hook cracks and fatigue cracks tend to fail in a ductile manner unless the base metal itself is prone to brittle fracture initiation or the fracture jumps into the bondline. Therefore, it may be appropriate in certain circumstances to use a ductile fracture model to predict their failure stresses. The Modified LnSec equation is one such model. Other models that likely would work equally well are PAFFC, CorLas™, or an API 579, Level II analysis.

5. The Modified LnSec equation when used with the base metal Charpy energy was found to give reasonable (and often over-conservative) predictions of the failure stress levels of 39 of 59 hook cracks.

6. The Modified LnSec equation when used with a Charpy energy of 15 ft lb was found to give reasonable (and often over-conservative) predictions of the failure stress levels of 31 of 32 fatigue-enlarged defects.

7. Where a hook crack resided in a brittle material or where the fracture of a hook crack jumped into the bondline of an LF-ERW, DC-ERW, or flash-welded seam, the Raju/Newman equation used with a toughness of level of 22.4 $ksi\sqrt{inch}$ (corresponding to a Charpy energy of 4 ft lb) was found to give lower-bound estimates of the failure stress.

8. The Raju/Newman equation is probably not a suitable model to use for calculating failure stress levels for fatigue-enlarged anomalies near ERW seams because such flaws tend to fail in a ductile mode.

9. The toughness of an ERW seam within a single piece of pipe can vary significantly from point to point along the seam.

10. The use of lower-bound estimates of failure stress is permissible for prioritizing ILI crack-tool anomalies for excavation and examination. Such lower-bound estimates are not appropriate for calculating the remaining lives of unexamined defects or defects that have barely survived a hydrostatic test. Appropriate methods for calculating remaining lives are being considered in a companion study under Subtask 2.5 of this project.

11. The use of lower-bound estimates or conservative models for predicting failure stress likely will result in excavations and examinations of many anomalies that are non-injurious along with those that are found to be injurious and need to be repaired.

Implications for Calculating the Failure Stress Levels of ERW Seam Anomalies Detected by ILI

As stated in the background section of this report, the primary mission of this study was to determine whether or not known models can be used to make reliable predictions of failure stress levels of defects in or adjacent to ERW seams. ILI tool service providers typically use a specific model and a single level of toughness to calculate the failure stresses for all detected and sized anomalies. Anomalies are then prioritized for excavation and examination on the basis of the calculated failure stresses. Pipeline operators and ILI tool service providers usually are faced with the problems that the toughness of the material is not known and that toughnesses are likely to vary from one batch of pipe to another and even along the seam of a single piece of pipe. In most situations the ILI tool service providers have no alternative but to assume a single level of toughness. Usually the assumed value will lead to predictions of elastic-plastic failure. This means that the possibility of brittle fracture is often overlooked.

As shown herein, cold welds and selective seam weld corrosion defects are prone to fail in a brittle manner, but hook cracks and fatigue-enlarged defects, more often than not, tend to fail in a ductile manner. So, even if the lengths and depths of anomalies were to be accurately portrayed by an ILI seam assessment, the list of calculated failure stress levels would not necessarily afford a reliable prioritization of the discovered anomalies. To overcome this situation the following improvement to ILI crack-detection technology should be sought.

It is important for ILI crack-detection technology to be able recognize the type of seam anomaly that is detected. The current categorizations used by ILI tool service providers: crack-like, notch-like, weld anomaly, and crack field are not useful in the context of ERW seam anomalies. Instead, the technology should be modified to identify and distinguish between bondline defects (cold welds and selective seam weld corrosion) and non-bondline defects (hook cracks, mismatched plate edges, damaged edges, and any anomaly that has been enlarged by pressure-cycle-induced fatigue). The following characteristics of each of these may provide clues as to how they might be distinguished from one another.

- Cold welds are tight cracks lying precisely along the bondline. In LF-ERW, DC-ERW, and flash-welded seams, they tend to be relatively small. In many cases they are short and deep and occur in a repetitive pattern. It is likely that because of the brittleness of the bondline regions in LF-ERW, DC-ERW, and flash-welded seams, large cold welds never survive the mill test and seldom, if ever, become enlarged by pressure-cycle-induced fatigue. The greatest threat they pose to pipeline integrity appears to be their propensity to cause leaks.
- Hook cracks do not coincide with the bondline. By definition, they are skelp defects that coincide with planes of inclusions that are curved during the upsetting process as the seam is formed. As a result, hook cracks tend to have a cross-sectional J-shape that should produce different responses to ultrasonic beams aimed from one side of the crack versus from the other side. Hook cracks also tend to be longer than cold weld defects. One challenge with respect to hook cracks is that hook cracks that lie very close to the bondline may not have much curvature. Also, there appears to be a risk when hook cracks that are close to the bondline start to grow. In such a case the fracture may jump to the bondline causing a sudden brittle failure at an unexpectedly low stress. This phenomenon is believed to have caused the 2007 failure of the Dixie Pipeline at Carmichael, MS.
- Selective seam weld corrosion usually is centered on the bondline. Unlike cold welds, however, selective seam weld corrosion tends to be wedge-shaped in cross section, making it somewhat of a volumetric defect. This should make it distinguishable from cold welds and hook cracks. One challenge would be to separate selective seam weld corrosion from other volumetric defects such as mismatched edges and damaged edges. One consideration is that selective seam weld corrosion often occurs in conjunction with corrosion of the nearby base metal. It may be feasible to positively identify selective seam weld corrosion by overlaying the results of crack-tool inspections with the results of metal loss inspections.

- Defects subject to enlargement by pressure-cycle-induced fatigue include hook cracks, mismatched plate edges, and damaged plate edges. In HF-ERW pipe where the bondline may by relatively ductile, it is possible for cold weld defects to be large enough to grow by fatigue. The characteristics of hook cracks are discussed above. Mismatched edges and damaged edges tend to be volumetric defects that do not lie on the bondline. For any of these kinds of defects to become enlarged by fatigue, it is necessary that they be relatively large. Experience suggests[xvi] that the lengths of fatigue cracks that have caused failures range from about $\sqrt{Dt}$ to $4\sqrt{Dt}$ where D is the diameter of the pipe and t is the wall thickness. The most common size associated with past ERW seam fatigue ruptures seems to be $>2\sqrt{Dt}$. For a 12.75-inch-OD by 0.250-inch-wall pipe, $2\sqrt{Dt}$ is 3.6 inches.

If ERW seam anomalies can be distinguished in this manner, then the lists of anomalies can be prioritized by treating those that could fail in brittle manner (i.e., cold welds, selective seam weld corrosion, small hook cracks lying very close to the bondline) separately from those that are likely to fail in a ductile manner (i.e., large hook cracks or any hook crack where the crack tip is not close to the bondline, mismatched plate edges, damaged plate edges). The failure stress levels of those that could fail in a brittle manner could be calculated via the Raju/Newman equation while those that would likely fail in a ductile manner could be calculated via a ductile fracture model such as the Modified LnSec equation.

Of course, there should be continued emphasis on improving the ability of the crack-detection technologies to provide accurate anomaly size data (i.e., lengths and depths). The current capability that relies on depth sizing by ranges of depth should not be regarded as good enough. More accurate reporting of defect depth would result in improved calculations of failure stresses.

Lastly, there is the problem of not knowing the toughness of each and every seam or the variations in toughness along the seam of a particular piece of pipe. Until or unless a solution arises to this problem, ILI tool service providers should consider prioritizing anomalies on the basis of lower-bound toughness values. This would be relatively easy if ductile fracture behavior could always be expected. Unfortunately, this is not the case for pipe materials with LF-ERW, DC-ERW, or flash-welded seams. A near-term solution for those materials that could be considered is as follows:

- Use the overlaying of crack-detection tool results with metal-loss tool results to separate selective seam weld corrosion from other seam anomalies.
- Evaluate selective seam weld corrosion (SSWC) anomalies separately using the Raju/Newman equation with a toughness of 5.2 $ksi\sqrt{inch}$ to prioritize the features.

- Evaluate short non-SSWC anomalies using the Raju/Newman equation with a toughness of 22.4 $ksi\sqrt{inch}$ to prioritize the features. A short anomaly could be defined as an anomaly less than or equal to $2\sqrt{Dt}$ in length. The rationale is that most cold welds are short.
- Evaluate long non-SSWC anomalies (>$2\sqrt{Dt}$ in length) using a ductile fracture model with a toughness corresponding to a full-size-equivalent Charpy upper shelf energy of 15 ft lb. The rationale is that long anomalies are the ones that are most likely to grow by pressure-cycle-induced fatigue.

APPENDIX A - BATTELLE'S EXPERIENCE IN PREDICTIONS OF FAILURE PRESSURE FOR ERW AND FLASH WELD SEAMS

Battelle
The Business of Innovation

October 3, 2012

Kiefner & Associates, Inc
585 Scherers Court.,
Worthington, Ohio
43085

RE: Input Concerning Interim Reporting for Contract DTPH56-11-T-000003
Comprehensive Study to Understand Longitudinal ERW Seam Failures

Dear: John

Battelle Memorial Institute, through its Corporate Operations (Battelle), is pleased to submit our input to your interim task report for the subject project titled ***Battelle's Experience in Predictions of Failure Pressure for ERW and Flash Weld Seams***. This input is for you use as you determine best suits the goals of the project and your subtask, with the possibility that parts of it might best be placed in an appendix.

Sincerely,

Brian Leis

Brian Leis
Sr. Research Leader
Energy Systems

Battelle
The Business of Innovation

Input to KAI Interim Reporting

Battelle's Experience in Predictions of Failure Pressure for ERW and Flash Weld Seams

By

B. N. Leis

Battelle Memorial Institute
505 King Avenue
Columbus, OH 43201

Prepared for use by Kiefner and Associates in regard to
Contract No. DTPH56-11-T-000003
U.S. Department of Transportation
Pipeline and Hazardous Materials
Safety Administration
1200 New Jersey Ave., SE
Washington DC 20590
Battelle Project No. G006084

October 3, 2012

Table of Contents

List of Figures

List of Acronyms and Symbols

API	American Petroleum Institute
CVN	Charpy vee-Notch
ERW	electric resistance weld
FW	flash weld
HAZ	heat affected zone
IM	integrity management
IMP	integrity management plan
ILI	in-line inspection
NTSB	National Transportation Safety Board
OD	outside diameter
PAFFC	pipeline axial flaw failure criterion
PHMSA	Pipeline and Hazardous Material Safety Administration
PTW	part-through-wall
PWHT	post-weld heat treatment
SATT	shear-area transition temperature
SMYS	specified minimum yield stress
SSC	selective seam corrosion
TW	through-wall
UTS	ultimate tensile stress

Executive Summary

Models that predict the response of defects to the effects of increasing pressure are the basis to determine the severity of anomalies and prioritize those considered defects, and also contribute to determining the timeline to respond. This report has evaluated the viability of the Battelle model known as PAFFC in applications to a range of ERW/FW defects, including cold welds, stitched welds, hook cracks, SSC, stress-corrosion cracking in the seam, and penetrators in combination with a cold weld relative to circumstances documented in Battelle's archival database for such defects.

It was found that if the defects were simple, and so can be easily sized and well represented by the idealizations used in the collapse and fracture models, and information was available to quantify the local resistance, then reasonable predictions of the failure behavior were achieved. For such cases the ratio of predicted to actual failure pressure was 0.94, with a coefficient of variation of just 0.13 – indicating a modestly conservative prediction of failure pressure and limited scatter. In contrast, for other cases among Battelle's library of 289 such failures where the circumstances are not well characterized, it was noted that the failure pressure was poorly predicted. This was illustrated in regard to poorly characterized cold welds, for which the ratio of predicted to actual failure pressure was 1.55, with a coefficient of variation of 0.31 – which indicates significant scatter. It was noted in this context that because such models are now used to size features, as well as to predict failure pressure, they must be accurate and precise – as a conservative failure pressure gives rise to a non-conservative defect size and related error in the re-inspection interval.

Because such models can be successful when the circumstances are reasonably known, the IM process that relies on such models can be effective if the gaps that lead to issues in predicting failure are bridged. In this context it was found that toughness must be quantified for the seam producer involved, and must be determined relative to the location of the defect – otherwise significant predictive errors can be anticipated. Likewise, the defect size must be reasonably quantified, with care taken where adjacent features can interact axially. Finally, the shapes and sizes of the features must be reasonably represented by the idealizations that underlie the plastic-collapse and/or fracture analysis.

Thus, as noted earlier there is a need to more broadly quantify the range of defect shapes both axially and through thickness, as well as in cross-section in regard to some defect types. In addition, there is a need for a library of properties relevant to pipe producers and defect locations known to be problematic. As some results are in hand to bridge gaps in regard to properties, but the usual idealizations in libraries of available fracture and collapse solutions fall short of the range of features that can be found in dealing with FW/ERW defects, it is recommended that work be initiated to bridge this analysis gap.

Battelle's Experience in Predictions of Failure Pressure for ERW and Flash Weld Seams

Introduction

Over the many decades Battelle has been engaged in work dealing with the transmission pipeline industry models have been developed to quantify the failure response of axial defects and cracks, such as occur along electric resistance welds (ERW) and flash weld (FW) seams. As time has passed each of those models have evolved to better address the range of steel toughness involved, as well as the nature of the defects and cracking that pose threats to the transmission pipeline industry.

Given the just-noted history, this report could trace the utility of the models and their evolution in regard to predictions of failure pressure made for ERW and FW seam failures in Battelle's database[(1)*], which reflects failures that occurred in pressure tests or during service. However, as it is clear from the experience gained over the decades that such predictions can be highly variable depending on what is known about the dimensions of the defect that controls failure, and the local properties, this report opens with discussion of factors controlling failure at ERW and FW seams, and thereafter focuses on predictions of cases where those factors could be reasonably quantified as inputs to the predictive process. Finally, those outcomes are contrasted to an example for which the necessary inputs were less well quantified.

Background

Role of Predictive Models

Regulatory mandates[(2,3)] establish the expectations for pipeline integrity management (IM) and direct its timeframes, while industry guidance[(e.g.,4,5)] identifies the nature and scope of plans that taken together are designed to meet those expectations. These plans integrate components that include: Integrity; Performance; (Continuous) Improvement; Communications; Change; and Quality.

The integrity component relies on an IM Plan (IMP) that at a high-level involves a cyclic process that steps through data gathering, and threats assessment and evaluation, which is followed by inspection and condition monitoring, integrity assessment to prioritize threats and set the response-timelines, and follow-up mitigation. Each of these steps adds to the database, which leads to a systems-wide resource that is integrated and aligned in space and time. The work scope developed by the Pipeline and Hazardous Material Safety Administration (PHMSA) in concert with the National Transportation Safety Board's (NTSB) guidance targets integrity assessment and the database that supports it. Specifically, this includes: 1) condition assessment, 2) the analysis of anomalies identified including their severity, and 3) prioritization of the defects and 4) the timeline to respond. Threat and anomaly severity are quantified relative to failure pressure, which makes clear their role in this IM process. Models that predict the response of defects to the effects of increasing pressure are the basis to determine the severity of anomalies and prioritize those considered defects, and contribute to determining the timeline to respond.

[*] Superscript numbers refer to the list of references compiled at the end of this report

Factors Controlling Failure

Models to predict failure at axial anomalies in transmission pipelines have been developed over the years at Battelle[6-9]. These models have been formulated with a basis in fracture mechanics, coupled with the realization that as the toughness increased there was a transition to flow-controlled failure or to collapse-controlled failure. These formulations quantified the severity of anomalies in terms of:

a) their physical dimensions (i.e., length, depth, area);
b) the dimensional properties of the pipe (diameter, thickness);
c) the flow properties of the pipe (yield and ultimate stress, strain hardening response);
d) the fracture properties of the pipe (fracture resistance based on Charpy v-notch (CVN) or J-based metrics); and
e) the operational/service conditions of the pipeline.

Anomalies that arise uniquely in regard to producing ERW and FW seams are indentified in API 5T1[10], which further distinguishes some features as being unique to the FW and ERW processes – although in some ways this distinction seems arbitrary and can be confusing[11]. The anomalies identified by API can be grouped as bondline and heat-affected zone (HAZ) defects. Bondline defects that develop during production include cold welds, weld-area cracks, stitched welds, inclusions, penetrators, and pinholes. Features that develop in or across the HAZ as noted in API 5T1[10] include hook cracks, inadequate or excessive flash trim, and contact marks/cracks. A second group of anomalies develop post-production, which arise due to in-service degradation or growth mechanisms, such as corrosion, selective seam corrosion (SSC), and fatigue.

When the formulation of the models is viewed relative to the nature of ERW and FW seam features, the response of such defects to increasing pressure in a given line-pipe geometry is found to depend on five key factors, which include[11]:

1. the feature's size and its axial and out-of-plane continuity with adjacent feature(s), which where features interact can be represented by their overall dimensions;
2. the mechanical (flow) and fracture properties local to the boundaries of the feature(s);
3. the pressure-induced hoop stress (which can in some service scenarios act in combination with other hoop-oriented stresses) relative to the specified minimum yield stress (SMYS);
4. whether the feature(s) is(are) blunt as occurs for penetrators (and by analogy those termed pinholes as defined by API 5T1[10]) or sharp as is typically the case for cold welds, weld-area cracks, and hook cracks, stitched welds that embed cold-weld segments, and SSC; and
5. the mechanism(s) driving growth, including possible axial coalescence between the tips of axially adjacent features.

The ensuing section illustrates the above factors in reference to the more prevalent bondline and HAZ defects that develop due to the seam process, and due to in-service growth mechanisms, such as SSC and fatigue.

Aspects of Failure at Select Types of Seam Defects

Reference 1 tabulates the circumstances associated with 289 failures culled from more than 80 reports, including several covering multiple retest failures. While failure predictions have been made for many of these, experience indicates that when fracture properties relevant to the failure are unknown, or poorly are characterized, the resulting predictions of failure pressure tend to scatter badly, from conservative to nonconservative. The same outcomes are evident when the physical size of the defect that originates the failure is difficult to quantify. This section briefly outlines aspects of select defect types as a guide to understand how to best idealize the defect and its resistance to failure.

Selective Seam Corrosion

As broadly illustrated in Reference 11, SSC can lead to defects that are simple in profile with a rather constant groove depth that is continuous along the length of the feature, where the adjacent surface of the pipeline's outside diameter (OD) is largely uncorroded. Likewise, SSC also can involve complex profiles due to corrosion along the V-groove that develops symmetrically or asymmetrically across the seam, which is far from uniform in depth and is axially discontinuous.

The formation of a V-groove due to SSC can trigger failure through the net-section, either by continued corrosion, or collapse- or fracture-controlled failure, depending on the properties of the seam, the hoop stress relative to SMYS, and the length and depth, and the axial continuity of adjacent grooving. In addition to failure through the root of the V-groove, or through the axial coalescence of adjacent V-grooves, SSC can lead to very localized narrow attack than can develop deep into the pipe wall from the root of the V-groove, creating crack-like features that pose a much greater integrity threat than the V-groove alone.

Where SSC presents a simple continuous V-groove profile of near-constant depth, as illustrated in Figure 1, these defects are among the easiest to predict relative to other more complex features. The depth profile can be reasonably sized using nondestructive methods, provided that crack-like selective attack has not occurred. Thereafter, mechanics solutions for grooves coupled with cross-weld strength properties in a net-section (plastic collapse) analysis can be quite accurate in such cases. While if crack-like selective attack has occurred the interface strength across the crack can be taken as zero, predicting the failure response of the net ligament remains a challenge because the properties of the seam are ill characterized below SSC. Cases where the features are axially discontinuous and interaction between the features can be assessed[e.g.,12] can be predicted – but the predictive process is much less certain.

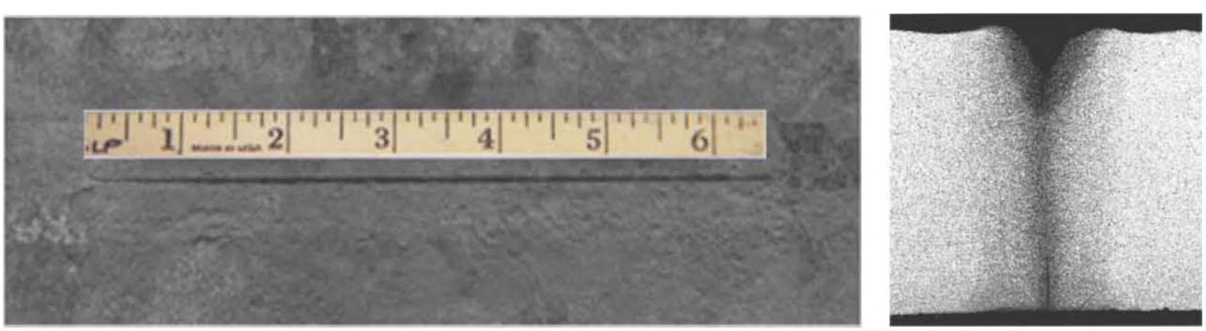

a) OD surface view of uniform SSC **b) typical transverse x-section: t = 0.312"**

Figure 1. SSC that reflect uniform seam attack absent significant surface corrosion

As noted elsewhere[11], aspects of the critique noted in regard to P-09-1 could be simply resolved for most SSC features by developing a library of collapse and fracture solutions for the practical range of such features – thereby facilitating viable integrity analysis. As in-line inspection (ILI) evolves to better detect and characterize all types of seam anomalies, the need for predictive tools will broaden to include prioritizing features, and choosing which to dig, and when.

Cold Welds, Hook Cracks, and Weld-Area Cracks

Prior discussion regarding cross-sections and photographs of fracture features dealing with cold welds and hook crack origins[11] indicates a range of complexity comparable to that evident for SSC. For example, in parallel to the simplest scenario for SSC, Reference 11 illustrates a simple part-through wall (PTW) hook crack origin that is continuous and smooth, both axially and into the thickness. One essential difference between SSC and a hook crack in this context is that the SSC produced a V-groove that absent crack-like selective attack is relatively blunt, whereas the hook crack can produce a geometrically sharp tip. This opens to the second essential difference, which reflects the observation that blunt features typically fail via plastic collapse, whereas sharp features tend to fail via fracture control in seams where the toughness is limited. In turn, this opens to the third essential difference: local toughness properties are needed to predict failure, rather than strength.

A PTW crack origin that is perpendicular to the pipe wall and is continuous and smooth, both axially and into the thickness, can be reasonably idealized using fracture mechanics – provided that the effect of axial profile idealized in fracture as semielliptical rather than a nearly constant depth is addressed when dealing with shorter features. In contrast, where such defects are long compared to their depth, other idealizations within the scope of available fracture theory can be used to approximate the failure response of this defect. Care must be taken to use fracture properties that are relevant to the location of the feature. Figure 2 illustrates the significant differences in toughness that can be seen at differing locations within an autogenous weld.

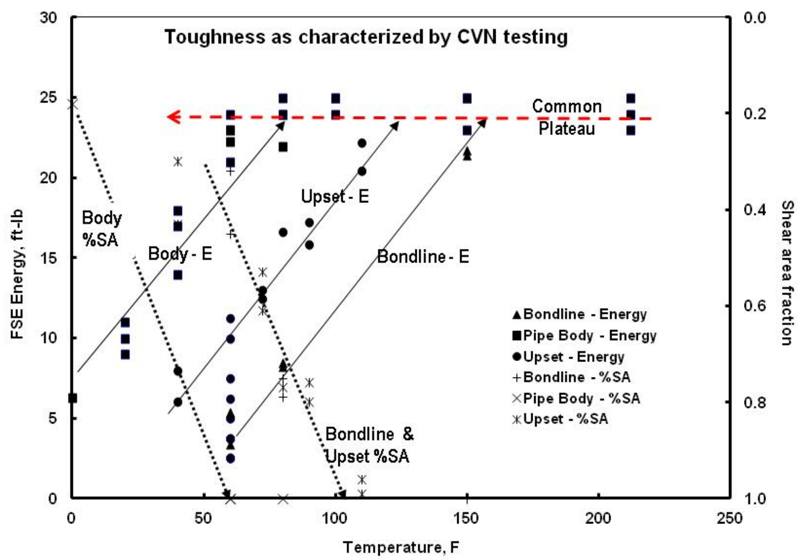

Figure 2. Differences in CVN resistance depending on the location in the seam[11]

Figure 2 reflects results developed by testing that centered the CVN notch in the bondline, or placed it in the upset/HAZ, and/or in the of pipe body. This testing practice indicates that the properties in the ERW/FW seam can fall well below typical body data, in regard to both the plateau and shear-area transition temperature (SATT). It is apparent there that the fracture resistance in the bondline is roughly 50% of that in the upset/HAZ, which in turn is roughly one-half of that of the pipe body. It is evident from Figure 2 that values of the full-size equivalent energy in the bondline can fall as low as a few foot-pounds. Testing done to quantify the fracture initiation resistance and the stable tearing resistance based on J-Tearing fracture theory are correspondingly low. Finally, Figure 2 shows that, as quantified by the CVN test practice that typically shows some scatter, the fracture morphology of the bondline and upset/HAZ are comparable, with a much higher SATT than the body, such that these areas will show more brittle fracture response at in-service temperatures.

As was noted in regard to SSC, hook cracks and cold welds, and related crack-like features can also be quite complex. Segments representing a combination of inadequate upset and inadequate heating can develop along a longitudinal FW/ERW seam in a variety of shapes, which can range from a shallow PTW feature to a TW defect. Adjacent features can lie on offset planes for hook cracks, whereas both hook cracks and cold welds/weld-area cracks can be discontinuous axially and across the width. The scope of this complexity is practically limited by the range of inadequate upset and heating that causes them. Thus, just as for SSC, the available technology for collapse and fracture analysis falls short of addressing this range of complexity. But as noted earlier in regard to SSC, the critique leveled by the NTSB in regard to P-09-1 can be simply resolved by developing a library of collapse and fracture solutions to bridge this gap. Because the range of generic shapes and sizes needed in regard for SSC parallels many of those needed for hook cracks and cold welds/weld-area cracks, work done to address SSC needs to broaden marginally to address the threat posed by these types of defects.

Fracture surfaces coupled with the related cross-sections provide insight into the strength and toughness of hook cracks and cold welds[11]. The upper-bound strength across a well made forge-welded seam should be equal the ultimate tensile strength (UTS) of the steel in the pipe body. In contrast, views of some cold welds indicate that the lower-bound strength across such welds is near zero. It follows that the strength across a bondline defect reflects the area that is bonded coupled with the quality of the bond. In turn, this means that the net-area that develops across this interface, coupled with the local strength and toughness are essential to make viable predictions of failure response. Such features can be short and shallow, but equally can be quite long. Where such features are complex, identifying the portion of the crack that is the origin can be difficult, which leads to uncertainty in predicted failure pressure. For pipe known to precede the use of a post-weld heat treatment (PWHT), bondline failures often occur in a hard zone that is due to the presence of untempered martensite. Upsets in the PWHT that lead to inadequate normalizing, and the presence of untempered martensite and high hardness likewise open to brittle response.

Fractography for hook cracks that lie perpendicular to the pipe surface suggests they too can have strength that ranges from zero over the cracked interface, to values approaching the UTS. As above, this means that the net-area that develops across this interface, coupled with the local strength and toughness can be essential to make effective predictions of failure response. Such features can be short and shallow, but equally can be quite long. As above, where such features are complex, identifying the portion of the crack that is the origin can be difficult, which leads to uncertainty in predicted failure pressure.

Stitched Welds, and Pinholes and Penetrators per API 5T1

The key to distinguishing a stitched weld from a cold weld is a good bond that is periodically separated by a poor bond. If the poor bond has zero strength, and the good bond full strength, and the stitching is uniform over its length, then a stitched weld has a lower-bound strength that corresponds to one-half the UTS. As the quality of the poor bond increases, a stitched weld can achieve an upper-bound strength equal to the UTS. Guided by these observations on strength, and some evidence of the bond quality, predictions can be made for stitched welds that on occasion can be quite accurate.

Pinholes and penetrators as defined relative to the supporting photographic images in API 5T1 are cylindrical features that lie across the pipe wall, whose length (diameter) is small relative to the wall thickness of the pipe. It is generally considered that such features develop through wall (TW), although this is not always the case. According to API 5T1, whether it is termed a pinhole or termed a penetrator depends on whether the feature lies across a FW seam (penetrator) or an ERW seam (pinhole). To be clear for present purposes, Figure 3 shows a view of what is often called an "oxide finger" in Battelle's reporting, which by virtue of its shape and the absence of any oxide could be either a penetrator or a pinhole. Battelle's database shows only a few failures where penetrators affected the seam strength sufficiently to cause failure in-service or at hydrotests pressure levels – in which case there was a cluster of such features. Given the interface strength between the oxide, or the strength of the oxide, when present, the strength of the weld is dictated by the net-section area and the quality of the bondline. Only retrospective predictions have been made for such features, with reasonable results achieved in such cases.

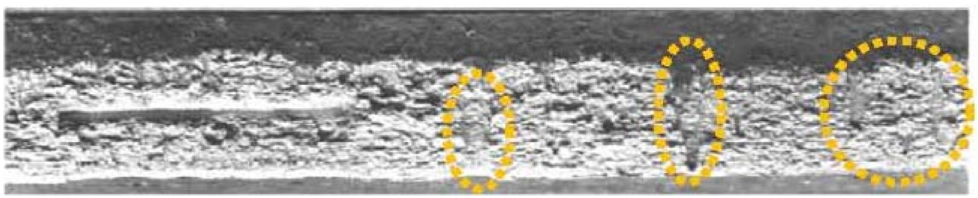

Figure 3. View illustrating the look of a penetrator or pinhole (below a PTW cold weld)

Summary

It is apparent that the shapes of cold welds, hook origins, and the other features considered can range from quite simple through very complex, running from PTW to TW. In some cases identifying the location and extent of the origin can be difficult, as can determining the portion of the defect that was activated to cause the failure. Moreover, in cases where the origin can be identified, characterizing its size, and representing the feature's shape using the idealized formats for which solutions currently exist, can likewise be problematic. A library of parametric mechanics and fracture analyses solutions would offset this concern. Once those aspects are better quantified, the interpretation algorithms and reporting schemes for ILI seam tools should be undated to embed such insights.

Limited bond strength can develop when the production process leads to inadequate upset, or inadequate heating, or both. In the worst case the weld is cold, and there is no interface to fail: so a crack exists as the pipe enters service. Varying degrees of inadequate heating or upset also can occur, which lead to a range of bond quality that the runs from near-zero strength up through the strength of the line-pipe. As such, failure can occur via plastic collapse at levels approaching the UTS, but at the other extreme of low bond strength net-section collapse can occur through a quite low-strength bond. While macroscopically little plastic deformation occurs in the low-strength cases, the failure process can be microscopically ductile. In contrast, even where a strong bond is achieved, the region of bondline can contain untempered marteniste, which forms because autogenous welds involve limited heat input and are subject to a large heat sink. Thus, a strong bond can fail in a macroscopically brittle manner at the mircoscale, and so show limited resistance to pressure.

It follows that, depending on how well the defect can be sized, and how well the properties local to the defect have been characterized, predictions of the failure pressure of defects that form in FW and ERW seams can run from conservative to nonconservative.

Reference 11 makes clear that identifying the initial size of even simple cold welds based on the "as-opened" appearance can lead to errors in actual length on the order of ~20%, because the oxides present mask aspects of the feature. For collapse-controlled failures, that work indicates that such an error leads to a 20% error in predicted pressure, while a 40% error in length causes a 40% error, and so on. Likewise, simple analysis for fracture controlled failure indicates a 20% error in defect length causes a 44% error in predicted pressure for a TW defect, with comparable results indicated for PTW features. As such, errors in defect sizes, shapes, and their continuity along and TW can cause significant errors affecting both predicted pressure (and re-inspection intervals).

As the next section shows, simpler features with well characterized properties can be predicted. However, because the extent of solutions is limited in dealing with the more complex features, and their sizes and shapes are ill-defined, such predictions can be challenging.

Model Predictions for FW and ERW Seam Defects

The Predictive Models

As noted earlier, the models to predict failure at axial defects in transmission pipelines developed at Battelle[(6-9)] have been formulated with a basis in fracture mechanics that has been coupled with the realization that as the toughness increased there was a transition to flow-controlled failure or to collapse-controlled failure. The initial model[(6,7)] was published in the early 1970s and is usually referred to as the NG-18 Equation, but it is also known as the log-secant equation because it is based on the empirical calibration of the semi-analytic log-secant model developed for axial defects in pipes by Hahn[(13)] at Battelle in 1969.

The chemistry and processing of line-pipe steel have evolved considerably since the mid to late 1960s, resulting in higher-strength grades that are both tough and weldable. This fact, coupled with problems in predicting failure of short and/or shallow defects, motivated the development of a second model that was formulated based on fracture theory and plastic-collapse principles, and so capable of characterizing failure of the steels of more recent manufacture without resort to empirical calibration. This resulted in the PRCI ductile flaw growth model[(8)], and PAFFC[(9)] – a failure criterion based on that model. In spite of its more general formulation[(e.g.,see14)], this model was validated initially using the database used to empirically calibrate the NG-18 Equation, and subsequently by a broad range of other full-scale test results that range up through modern Grade X80[(e.g.,see15)]. This report deals with predictions based on the most recent of these formulations.

Simple Well Characterized Defects

PAFFC has been used to predict the failure response of simple seam-weld features that reflect SSC, cold welds, hook cracks, stitched welds, and penetrators/pinholes found in combination with other bondline defects. Cases where predictions are made reflect circumstances where the client involved is interested in completing this type of analysis, such that data are developed as needed to support the analysis, as for example that shown in Figure 2, or where results were already developed for a given seam type / producer and approximate pipe vintage. While PAFFC predicts failure in regard to both plastic-collapse and toughness-controlled modes of failure, in cases where toughness was not anticipated to control the failure the predictions were typically made without generating otherwise unnecessary fracture-resistance data. In all other cases, the flow and fracture properties were developed or existed as needed to represent the conditions local to the seam defect.

Figure 4 summarizes the results of such predictions, which are presented there on the y-axis as a function of the actual failure pressure shown on the x-axis. It is evident from the pressure levels involved that these data represent a mix of pressure-test results and in-service cases.

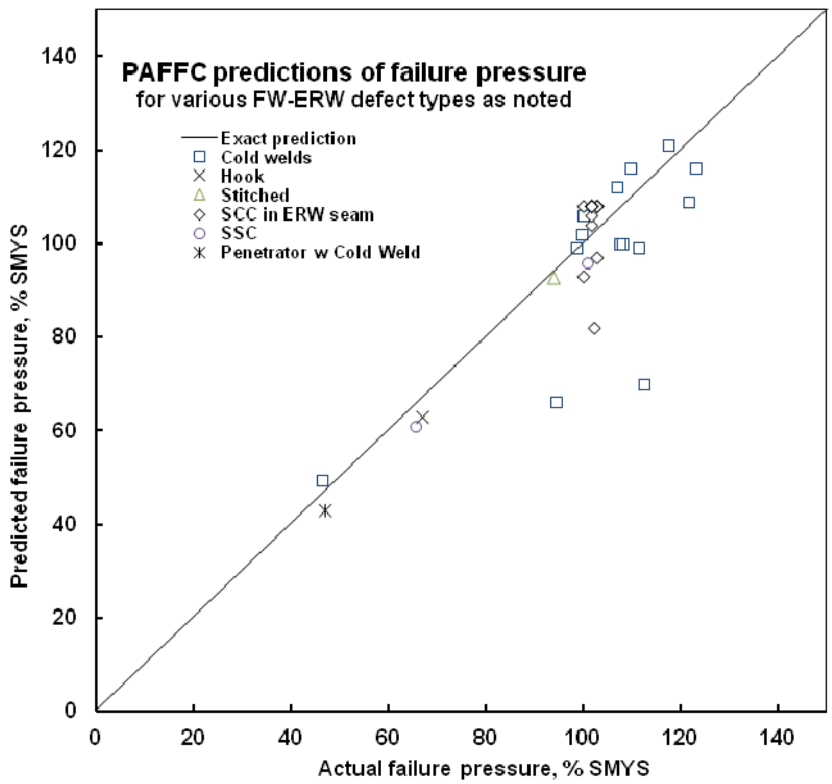

Figure 4. Comparison of predicted failure response with the actual response

It can be seen in reference to Figure 4 that if the defects are simple, and so can be easily sized and appropriately represented by the idealizations used in the collapse and fracture models, and information is available to quantify the local resistance, then reasonable predictions of the failure behavior can be achieved. The ratio of predicted to actual failure pressure is 0.94, with a coefficient of variation of 0.13, which indicates a modestly conservative prediction of failure pressure and limited scatter. This outcome would be much improved if the two predictions that involved axially discontinuous cold welds that fall well below the 1:1 trend in Figure 4 were excluded. While it might be argued that these predictions are quite acceptable because they are conservative, it must be emphasized that a conservative prediction of failure pressure leads to a non-conservative prediction in the corresponding defect size, and an equally non-conservative prediction of the re-inspection interval.

It follows that models to predict failure pressure as a function of defect size must strive for accuracy and precision rather that conservatism – which is in strong contrast to the conservatism sought prior to the need for defect sizing that is central to setting re-inspection intervals.

Poorly Characterized Defects

In deference to the quality outcomes evident in Figure 4, for other cases among Battelle's library of 289 where the circumstances are not well characterized such failures cannot be predicted with anything close to the same degree of success. For example, if the toughness of the pipe body is taken as an upper-bound value to what can be anticipated in the bondline, then the ratio of predicted to actual failure pressure is 1.55, with a coefficient of variation of 0.31. The largest conservative prediction exceeds the actual outcome by more than a factor of two, whereas the worst non-conservative outcome errs by about 25%. On the other hand, if a bondline toughness level like that evident in Figure 2 is taken as typical of the local fracture resistance, the predicted failure pressure drops on average to values more consistent with the actual results, but the extent of the scatter remains high – with a comparable coefficient of variation near 0.30. It follows that using a more representative toughness leads to an improvement in predictions, but this does little to offset the scatter – which evidently reflects uncertainty in quantifying the shape and size of the features involved in the manner assumed by the fracture and collapse theories that underlie PAFFC. As all such models embed the same basic mechanics, similar outcomes are anticipated across the scope of those developed to date.

Consideration was given to assessing the relative drivers for inaccurate predictions based on the five key factors noted earlier as controlling the failure of seam defects. However, because in general two or more factors are typically unknown for most such cases, the understanding that derives from such efforts remains speculative or presumptive. Analytically bounding their role is also problematic, as this requires knowing which factors contribute in combination, and in what balance. Accordingly, the relative significance of some of the individual factors has been assessed follows. Where the toughness is unknown, predictions over a range of potentially relevant toughness can differ by 30%, or more. Likewise, where defect size is uncertain, particularly where adjacent features can interact axially, it is clear that predictions can err to the same extent. Finally, where the shapes and sizes of the features are not well represented by the idealizations commonly available for plastic-collapse and/or fracture analysis, significant uncertainty can enter in regard to the best approach to idealize the feature, leading to errors of that same order.

Thus, as noted earlier there is a need to more broadly quantify the range of defect shapes both axially and through thickness, as well as in cross-section in regard to some defect types. In addition, there is a need for a library of properties relevant to pipe producers and defect locations known to be problematic. Some results are in hand to bridge gaps in regard to properties(14), but as yet the usual idealizations in libraries of available fracture and collapse solutions fall short of the range of features that can be encountered in dealing with FW/ERW defects.

Summary, Conclusions, and Recommendations

Models that predict the response of defects to the effects of increasing pressure are the basis to determine the severity of anomalies and prioritize those considered defects, and also contribute to determining the timeline to respond. This report has evaluated the viability of the Battelle model known as PAFFC in applications to a range of ERW/FW defects, including cold welds, stitched welds, hook cracks, SSC, stress-corrosion cracking in the seam, and penetrators in combination with a cold weld relative to circumstances documented in Battelle's archival database for such defects[(11)].

It was found that if the defects were simple, and so can be easily sized and well represented by the idealizations used in the collapse and fracture models, and information was available to quantify the local resistance, then reasonable predictions of the failure behavior were achieved. For such cases the ratio of predicted to actual failure pressure was 0.94, with a coefficient of variation of just 0.13 – indicating a modestly conservative prediction of failure pressure and limited scatter. In contrast, for other cases among Battelle's library of 289 such failures where the circumstances are not well characterized, it was noted that the failure pressure was poorly predicted. This was illustrated in regard to poorly characterized cold welds, for which the ratio of predicted to actual failure pressure was 1.55, with a coefficient of variation of 0.31 – which indicates significant scatter. It was noted in this context that because such models are now used to size features, as well as to predict failure pressure, they must be accurate and precise – as a conservative failure pressure gives rise to a non-conservative defect size and related error in the re-inspection interval.

Because such models can be successful when the circumstances are reasonably known, the IM process that relies on such models can be effective if the gaps that lead to issues in predicting failure are bridged. In this context it was found that toughness must be quantified for the seam producer involved, and must be determined relative to the location of the defect – otherwise significant predictive errors can be anticipated. Likewise, the defect size must be reasonably quantified, with care taken where adjacent features can interact axially. Finally, the shapes and sizes of the features must be reasonably represented by the idealizations that underlie the plastic-collapse and/or fracture analysis.

Thus, as noted earlier there is a need to more broadly quantify the range of defect shapes both axially and through thickness, as well as in cross-section in regard to some defect types. In addition, there is a need for a library of properties relevant to pipe producers and defect locations known to be problematic. As some results are in hand to bridge gaps in regard to properties, but the usual idealizations in libraries of available fracture and collapse solutions fall short of the range of features that can be found in dealing with FW/ERW defects, it is recommended that work be initiated to bridge this analysis gap.

References

1. Anon., Annex A in Leis, B. N. and Nestleroth, J. B., "Battelle's Experience with ERW and Flash Weld Seam Failures: Causes and Implications," Interim Final Report on Task 1.4, Contract No. DTPH56-11-T-000003, September 2012.
2. Anon., Subpart O of Part 192 (Transportation of Natural and other Gas by Pipeline) of Title 49 of the CFR.
3. Anon., Section 195.452 of Subpart F and Appendix C of Subpart H in Part 195 (Transportation of Hazardous Liquids by Pipeline) of Title 49 of the CFR.
4. Anon., ASME B31.8S Managing System Integrity of Gas Pipelines, American Society for Mechanical Engineers, June 2010.
5. Anon., API Standard 1160, Managing System Integrity for Hazardous Liquid Pipelines, American Petroleum Institute, November 2001
6. Kiefner, J. F., Maxey, W. A., Eiber, R. J. and Duffy, A. R., "Failure Stress Levels of Flaws in Pressurized Cylinders," Progress in Flaw Growth and Fracture Toughness Testing, ASTM STP 536, American Society for Testing and Materials, 1974, pp. 461-481: see also Maxey, W. A., Kiefner, J. F., Eiber, R. J., and Duffy, A. R., "Ductile Fracture Initiation, Propagation and Arrest in Cylindrical Vessels," ASTM STP 514, American Society for Testing and Materials, Philadelphia, PA, 1972, pp. 70-81.
7. Kiefner, J. F., Maxey, W. A., and Eiber, R. J., "A Study of the Causes of Failures of Defects That Have Survived a Prior Hydrostatic Test", NG-18 Report No 111, 1980.
8. Leis, B. N., Brust, F. W., and Scott, P. M., "Development and Validation of a Ductile Flaw Growth Analysis for Gas Transmission Line Pipe," NG-18-193, 1991(PRCI L51543): see also Brust, F. W. and Leis, B. N., "A New Model for Characterizing Primary Creep Damage," International Journal of Fracture, Vol 54, pp. 45-63, 1992: see also Brust, F. W. and Leis, B. N., "A Study of Primary Creep Crack Growth At Room Temperatures," Proc. of the 5th International Conference on Numerical Methods in Fracture Mechanics, ed. A. R. Luxmoore, and D. R. J. Owen, Freiburg, FRG, pp. 321-332, 1990.
9. Leis, B. N. and Eiber, R. J., "Fracture Control Technology for Transmission Pipelines," Final Report on PR-003-084506, August 2008: see also Leis, B. N., "Hydrostatic Testing of Transmission Pipelines: When It Is Beneficial and Alternatives When It Is Not", PRCI Final Report PR 3-9523, 2002.
10. Anon., "API Bulletin on Imperfection Technology," API Bul. 5T1 (R2010), 2010
11. Leis, B. N. and Nestleroth, J. B., "Battelle's Experience with ERW and Flash Weld Seam Failures: Causes and Implications," Interim Final Report on Task 1.4, Contract No. DTPH56-11-T-000003, September 2012.
12. Stonesifer, R. B., Brust, F. W., and Leis, B. N., "Mixed Mode Stress Intensity Factors for Interacting Semi-Elliptical Surface Cracks in a Plate", *Engineering Fracture Mechanics*, Vol. 45, No. 3, pp. 357-380, 1993.
13. Hahn, G. T., Sarrate, M. and Rosenfield, A.R., "Criteria for Crack Extension in Cylindrical Pressure Vessels", *I J Frac Mech*, Vol.5, 1969, pp. 187-210.
14. Hart, B. O., Brongers, M. P. H., Bubenik, T., and Vieth, P. H., "Early Generation Seam Welds," Final Report R3017-01R, DOT-OPS/PRCI, January 2004.

APPENDIX B - THE MODIFIED LNSEC EQUATION AND THE RAJU/NEWMAN EQUATION

Modified LnSec Equation

$$\sigma_{fs} = \left(\frac{\bar{\sigma}}{M_P}\right)\cos^{-1}\left(e^{-x}\right)/\left(\cos^{-1}\left(e^{-y}\right)\right)$$

Equation ML 1

$$x = \left(\frac{12\dfrac{\mathrm{CVN}}{\mathrm{A_c}}\mathrm{E}\pi}{8\mathrm{c}\bar{\sigma}^2}\right)$$

Equation ML 1a

$$y = \left(\frac{12\dfrac{\mathrm{CVN}}{\mathrm{A_c}}\mathrm{E}\pi}{8\mathrm{c}\bar{\sigma}^2}\right)\left(1-\left(\frac{d}{t}\right)^{0.8}\right)^{-1}$$

Equation ML1b

$$\mathrm{M_P} = \left[\frac{1-\left(\dfrac{\mathrm{A}}{\mathrm{A_o}}\right)\left(\dfrac{1}{\mathrm{M_T}}\right)}{1-\left(\dfrac{\mathrm{A}}{\mathrm{A_o}}\right)}\right]$$

Maxey's Surface Flaw Equation

$$\mathrm{M_T} = \left(1+1.255\frac{\mathrm{c}^2}{\mathrm{Rt}}-0.0135\frac{\mathrm{c}^4}{\mathrm{R}^2\mathrm{t}^2}\right)^{\frac{1}{2}}$$

The Folias Equation for $c \leq 5\sqrt{Rt}$

$$M_T = 3.3+0.032\frac{L^2}{Dt}$$

The Folias Equation for $c > 5\sqrt{Rt}$

where:

σ_{fs}	is the hoop stress at failure for the surface flaw, psi

$$\bar{\sigma} = \sigma_{YS} + 10{,}000 \text{ psi}$$

σ_{YS}	is the yield strength of the material, psi
2c	is the length of the surface flaw, inches
R	is the radius of the pipe, inches
t	is the wall thickness of the pipe, inch
d	depth of defect, inch
A_o	= 2ct, in^2
A	is the area of the surface defect (i.e., 2cd if the flaw has uniform depth, d), in^2
E	Elastic modulus of the material
CVN	is the upper shelf energy as determined from tests of Charpy V-notch impact specimens

When the defect has a rectangular area, A becomes 2cd, so A/A_o becomes d/t. In most circumstances and for all the calculations used herein, the "Elliptic c-equivalent" format of the equation is used. In this format the area A is calculated as $2c_{eq}d$ and A_o is calculated as $2C_{eq}t$, so that A/A_o is equal to d/t. $2c_{eq}$ is equal to $\pi L/4$ where d, t, and L are defined in the diagram below. $2c_{eq}$ is then used in place of 2c in the Folias equation.

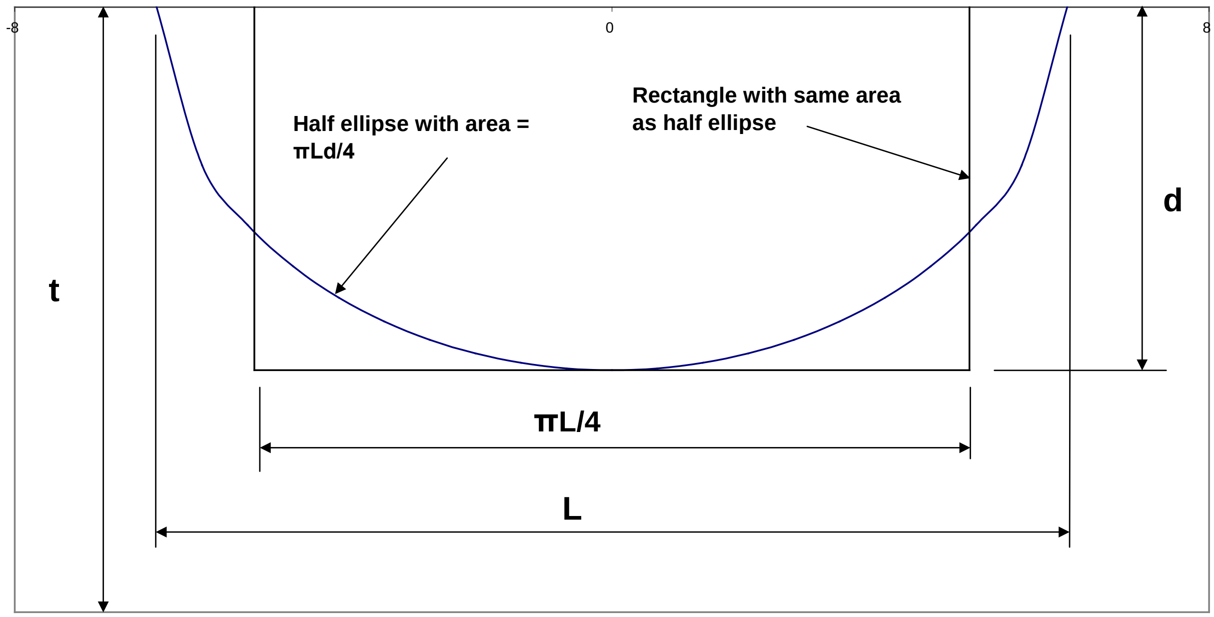

The Raju/Newman Equation for a Longitudinal Surface Crack in a Cylinder

Taken from the DTD Handbook(online @
www.afgrow.net/applications/**DTDHandbook**/sections/page4_2_2.aspx
Section 11.3, Tables 11.3.4 and 11.3.1)

In all cases used herein *a/c*<1 where *a* is the depth of the surface crack and *c* is half of its length. Note the definitions of *a*, *c*, ø, and *t* in the diagram below.

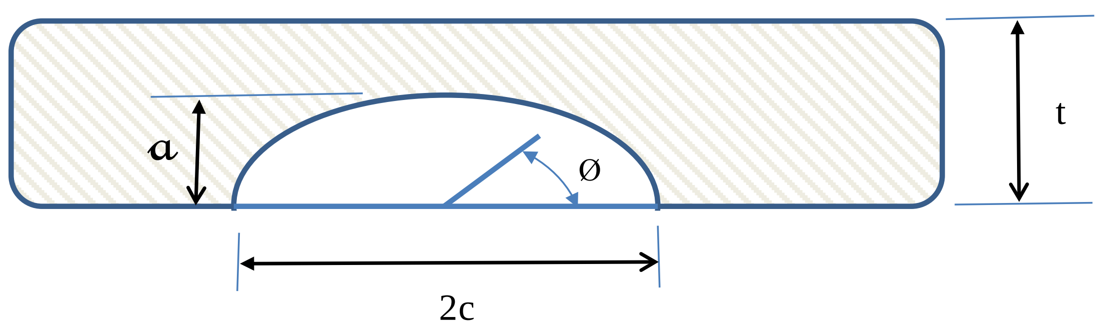

$$K_0 = F_0 \sigma_0 \sqrt{\pi a} \qquad \textbf{Equation RN 1}$$

$$F_0 = 0.97 M_0 g_1 f_\emptyset f_c f_i f_x \qquad \textbf{Equation RN 1a}$$

$$M_0 = m_1 + m_2 \left(\frac{a}{t}\right)^2 + m_3 \left(\frac{a}{t}\right)^4 \qquad \textbf{Equation RN 1b}$$

$$m_1 = 1.13 - 0.09 \left(\frac{a}{c}\right) \qquad \textbf{Equation RN 1c}$$

$$m_2 = -0.54 + \frac{0.89}{[0.2 + (a/c)]} \qquad \textbf{Equation RN 1d}$$

$$m_3 = 0.5 - \frac{1}{[0.65 + (a/c)]} + 14[1 - (a/c)]^{24} \qquad \textbf{Equation RN 1e}$$

$$g_1 = 1 + \left[0.1 + 0.35 \left(\frac{a}{t}\right)^2\right] (1 - \sin \emptyset)^2 \qquad \textbf{Equation RN 1f}$$

$$f_\emptyset = \left[\left(\frac{a}{c} \cos \emptyset\right)^2 + \sin^2 \emptyset\right]^{1/4} \qquad \textbf{Equation RN 1g}$$

Note that g_1 and $f_\emptyset$ are equal to 1 when Ø is 90° (the deepest point of the crack and the location of interest herein).

$$f_c = \left[\frac{(1+k^2)}{(1-k^2)} + 1 - 0.5\sqrt{\nu}\right] \left[\frac{2t}{D-2t}\right] \qquad \textbf{Equation RN 1h}$$

$$f_i = 1.0 \text{ for an internal crack}$$
$$f_i = 1.1 \text{ for an external crack}$$

$$f_x = \left[1 + 1.464 \left(\frac{a}{c}\right)^{1.65}\right]^{-\frac{1}{2}} \qquad \textbf{Equation RN 1i}$$

where:

σ_0 is the hoop stress , psi

K_0 is the stress intensity factor, psi$\sqrt{inch}$

Note that the hoop stress at failure of a surface crack is calculated by Equation RN1 when K0 is equal to the fracture toughness of the material.

Intentionally blank

REFERENCES

[i] Kiefner, J.F., and Kolovich, K.M., "*ERW and Flash Weld Seam Failures*" Subtask 1.4 of U.S. Department of Transportation Other Transaction Agreement No. DTPH56-11-T-000003, May 30, 2012.

[ii] Kiefner, J.F., Maxey, W.A., Eiber, R.J., and Duffy, A.R., "Failure Stress Levels of Flaws in Pressurized Cylinders", Progress in Flaw Growth and Fracture Toughness Testing, ASTM STP 536, American Society for Testing and Materials, pp 461 – 481, 1973.

[iii] Leis, B. N., Brust, F. W., and Scott, P.M., "Development and Validation of a Ductile Flaw Growth Analysis for Gas Transmission Line Pipe", Final Report to American Gas Association, NG-18, Catalog No, L51543, 1991.

[iv] Anderson, T. L., Merrick, R. D., Yukawa, S., Bray, D. E., Kaley, L., and Van Scyoc, K., "*Fitness-For-Service Evaluation Procedures For Operating Pressure Vessels, Tanks, And Piping in Refinery And Chemical Service*", FS-26, Consultants' Report, MPC Program On Fitness-For-Service, Draft 5, The Materials Properties Council, New York, N.Y., October, 1995.

[v] Harrison, R. P., Loosemore, K., and Milne, I., "*Assessment of the Integrity of Structures Containing Defects.*" CEGB Report R/H/R6. Central Electricity Generating Board, United Kingdom, 1976.

[vi] Jaske, C. E., and Beavers, J. A., "Development and Evaluation of Improved Model for Engineering Critical Assessment of Pipelines", Proceedings of IPC 2002, 4th International Pipeline Conference, September 29-October 3, 2002, Calgary, Alberta, Canada

[vii] J.C. Newman, Jr. and I.S. Raju, "An Empirical Stress-Intensity Factor Equation for the Surface Crack". *Engineering Fracture Mechanics,* Vol. 15, No. 1-2, pp 185-192, 1981, printed in Great Britain.

[viii] Eiber, R.J., Hein, G.M., Duffy, A.R., and Atterbury, T.J., "Investigation of the Initiation and Extent of Ductile Pipe Rupture", Report No. BMI-1793, Progress Report for May-December, 1966, U.S. Atomic Energy Commission Contract No. w-7405-eng-92, January 1, 1967.

[ix] Eiber, R.J., Maxey, W.A.., Duffy, A.R., and Atterbury, T.J., "Investigation of the Initiation and Extent of Ductile Pipe Rupture", Report No. BMI-1866, U.S. Atomic Energy Commission Contract No. w-7405-eng-92, NTIS, July 1969.

[x] Folias, E.S., "The Stresses in a Cylindrical Shell Containing an Axial Crack", Aerospace Research Laboratories, ARL 64-174, (October 1964).

[xi] Dugdale, D.S., "Yielding in Steel Sheets Containing Slits.", *Journal of the Mechanics and Physics of Solids*, Vol. 8, 1960, pp. 100 – 104.

[xii] Kiefner, J.F., “Modified equation helps integrity management”, Oil and Gas Journal, Oct 6, 2008, pp 76-82 and “Modified Ln-Secant equation improves failure prediction” Oct 13, 2008, pp 64-66.

[xiii] Griffith, A.A., “The Phenomena of Rupture and Flow in Solids”, *Philosophical Transactions*, Series A, Vol. 221, 1920, pp. 163 – 198.

[xiv] Irwin, G.R., “Analysis of Stresses and Strains near the End of a Crack Traversing a Plate”, *Journal of Applied Mechanics*, Vol. 24, 1957, pp. 361 – 364.

[xv] Barsom, J.M., and Rolfe, S.T., *Fracture and Fatigue Control in Structures: Applications of Fracture Mechanics*, Third Edition, ASTM Stock Number MNL41, 1999.

[xvi] Kiefner, J.F., Kolovich, C.E., Zelenak, P.A., and Wahjudi, T., “Estimating Fatigue Life for Pipeline Integrity Management”, IPC04-0167, *Proceedings of IPC 2004 International Pipeline Conference*, Calgary, Alberta, Canada (October 4-8, 2004).